POLITECNICO DI MILANO

Scuola di Ingegneria Industriale e dell'Informazione

Corso di Laurea Magistrale in

INGEGNERIA ENERGETICA - ENERGY ENGINEERING

APPLICATION OF ADM1 TO FULL-SCALE DIGESTER IN VIEW OF DIGESTION SCENARIOS

Master Thesis by **Alice Previati**

matr. 876019

Supervisor **Prof. Elena Ficara**

Co-supervisor **Eng. Arianna Catenacci**

Academic Year 2018-2019

Dedicato a mio papà,
perché sia orgoglioso di sua figlia grande,
per sempre

TABLE OF CONTENTS

Abstract in italiano **1**
Abstract **2**
CHAPTER 1. INTRODUCTION **3**
1.1 Processing and treatment of sludges with AD 6
1.2 Objectives 10
CHAPTER 2. LITERATURE REVIEW **12**
2.1 Energy consumptions and sustainability of WWTPs 12
2.2 Anaerobic codigestion in WWTPs 13
2.3 AD process modelling 19
2.4 Anaerobic Digestion Model nr. 1 21
2.4.1 ADM1 limitations 25
CHAPTER 3. MATERIALS AND METHODS **27**
3.1 Samples origin 27
3.2 Conventional analyses 29
3.3 Lipids, proteins and carbohydrates analyses 30
3.4 Hydrolysis techniques 31
3.5 Anaerobic biodegradability and activity tests 32
3.5.1 Specific Methanogenic Activity test 33
3.5.2 Biochemical Methane Potential test 33
3.6 Implementation of the ADM1 35
CHAPTER 4. RESULTS AND DISCUSSION **37**
4.1 Conventional analyses 37
4.1.1 VFA analyses 39
4.2 Lipids, proteins and carbohydrates analyses 41
4.3 Hydrolysis techniques 41
4.4 Anaerobic biodegradability and activity tests 45
4.4.1 Specific Methanogenic Activity tests 45
4.4.2 Biochemical Methane Potential tests 46
4.5 Implementation of the ADM1 51

CHAPTER 5. CONCLUSIONS AND PERSPECTIVES 57
Ringraziamenti 60
Bibliography 61
Appendix A 64
Appendix B 68
Appendix C 69
Appendix D 72

LIST OF FIGURES

Figure 1.1 Flowchart of the simplified AD process 9
Figure 1.2 Flowchart of the steps that have been adopted to calibrate the model of the full-scale digester 11
Figure 2.1 Flowchart of a detailed AD process 23
Figure 3.1 Satellite view of the WWTP under study 28
Figure 3.2 The WWTP under study: on the left, the pre-thickening unit; on the right, one of the anaerobic reactors 28
Figure 3.3 Set-up of the experiments run with the system AMPTS II; on the left, the thermostatic bath; in the middle, the absorption unit; on the right at the back, the measuring unit 33
Figure 3.4 User interface of the AQUASIM 2.0 platform 35
Figure 4.1 Correlation curves for the conversion of the VFAs concentration by gas chromatograph to VFAs concentration by test in kit 40
Figure 4.2 Measurements of the total carbohydrate concentration of the same sample that have been hydrolysed by different methods 43
Figure 4.3 Cumulative gross methane production during the SMA test; the dashed lines identify the interval of time in which the SMA value was evaluated 45
Figure 4.4 Plot chart of the cumulative net methane production in the BMP test with glucose as substrate (above); specific methane production rate (below) 47
Figure 4.5 Plot chart of the cumulative net methane production in the BMP test with cellulose as substrate (above); specific methane production rate (below) 48
Figure 4.6 Plot chart of the cumulative net methane production in the BMP test with yogurt as substrate; it can be noticed that the test of one bottle stopped earlier 49
Figure 4.7 Specific methane production rate 50
Figure 4.8 Plot chart of the cumulative net methane production in the BMP test with cellulose as substrate 50
Figure 4.9 Biogas production in the year 2016 according to the simulation in AQUASIM 55
Figure 4.10 Values of inhibition factors in the simulation of the liquid phase of reactor B 55

LIST OF TABLES

Table 1.1 Standards for the discharge from urban wastewater treatment plants (91/271/CEE) 4
Table 2.1 Some of the solutions that have already been applied to improve the exploitation of the energy content of wastewater, and so the efficiency of the WWTP 13
Table 2.2 Typical values of the Methane Yield from batch tests found in literature 16
Table 4.1 Characterisation of the samples: a = collected in April 2019; b = collected in June 2019 38
Table 4.2 Stoichiometric coefficients used for the COD conversion 39
Table 4.3 Coefficients of the linear regression fits built comparing the absolute VFA concentrations and the corresponding ones measured by the test in kit 40
Table 4.4 Results of the tests on the sensitivity of the hydrolysis pre-treatment; the method number is referred to the list that can be found in Materials and Methods 42
Table 4.5 Summary of the analyses on carbohydrates of the collected samples in June 2019 43
Table 4.6 Summary of the analyses on proteins of the collected samples in June 2019 44
Table 4.7 Summary of the analyses on lipids of the collected samples in April 2019 44
Table 4.8 Average nutritional values of a set of yogurt samples 44
Table 4.9 Results of the SMA test 45
Table 4.10 Methane yields resulting from the BMP test with glucose as substrate 47
Table 4.11 Methane yields resulting from the BMP test with cellulose as substrate 48
Table 4.12 Methane yields resulting from the BMP tests with yogurt and pre-thickened sludge 51
Table 4.13 Disintegration coefficients: a = Batstone et al., "Anaerobic Digestion Model No.1 (ADM1) IWA Scientific and Technical Report No. 13" (2002); b = Rosén and Jeppsson, "Aspects on ADM1 implementation within the BSM2 framework" (2006) 53
Table 4.14 Sizing of the full-scale digester in the WWTP under study 53

Table A. 1 Acid-base equilibria algebraic equation set 64
Table A. 2 Biochemical rate coefficients ($v_{i,j}$) and the kinetic rate equations (ρ_j) for soluble components (i = 1-12) 66
Table A. 3 Biochemical rate coefficients (vi,j) and the kinetic rate equations (ρj) for particulate components (i = 13-24) 67

Table B. 1 Ingredients of mother solution A 68
Table B. 2 Ingredients of mother solution B 68

Table B. 3 Ingredients of mother solution C 68

Table C. 1 ADM1 benchmark model, stoichiometric parameter values (on the left of the table) and biochemical parameter values (on the right) 69
Table C. 2 ADM1 benchmark model, physiochemical parameter values; Van't Hoff temperature correction has been applied if required 70

LIST OF ABBREVIATIONS

AcoD	Anaerobic co-digestion
AD	Anaerobic digestion
ADM1	Anaerobic Digestion Model nr.1
BMP	Biochemical methane potential
BOD	Biochemical oxygen demand
BOD_5	5 Days biochemical oxygen demand
CH	Carbohydrates
C/N	Carbon-to-nitrogen ratio
COD	Chemical oxygen demand
FM	Fresh matter
FW	Food waste
HRT	Hydraulic retention time
ISR	Inoculum-to-substrate ratio
LI	Lipids
OFMSW	Organic fraction of Municipal solid waste
OLR	Organic loading rate
PE	Population equivalent
PR (PT)	Proteins
sCOD	Chemical oxygen demand of soluble fraction
SRT	Solid retention time
SS	Sewage sludge
TKN	Total Kjeldhal Nitrogen
TS	Total solids
TSS	Total suspended solids
VFA	Volatile fatty acids
VS	Volatile solids
WWTP	Wastewater treatment plant

Abstract in italiano

La fase conclusiva delle acque reflue ha sempre ricevuto grande attenzione a causa della loro nocività per l'uomo e l'ambiente. Il trattamento delle acque reflue è un sistema complesso costituito da più passaggi, che richiedono tempo ed energia. Soprattutto nei Paesi sviluppati, gli impianti di trattamento delle acque reflue sono diventati importanti entità nella domanda nazionale di elettricità. Pertanto, il processo di digestione anaerobica dei fanghi ha acquisito grande importanza. Il suo funzionamento può essere ottimizzato in diversi modi. Tra questi, la co-digestione anaerobica è molto interessante perché consente di raggiungere tre obiettivi contemporaneamente: lo sfruttamento dei reattori anaerobici sovradimensionati, che si riflette sia in un aumento della produzione di biogas che in una diminuzione del costo specifico del processo; miglioramento delle condizioni del sistema anaerobico, che si riflette sia nell'aumento della produzione di metano e di biogas; possibile recupero di rifiuti, come OFMSW, rifiuti alimentari e sottoprodotti caseari. Tuttavia, la co-digestione anaerobica è un sistema ragionevole che dovrebbe essere gestito in modo adeguato. La modellazione è uno strumento utile per comprendere i processi biologici che si verificano durante il trattamento anaerobico, e quindi per migliorare le loro prestazioni.

In questa tesi, la simulazione di un digestore in scala reale per mezzo del modello ADM nr. 1 del gruppo di lavoro dell'International Water Agency è stato studiato. La piattaforma AQUASIM 2.0 è stata utilizzata per implementare la simulazione. I campioni raccolti nell'impianto studiato sono stati caratterizzati completamente. Molte difficoltà sono state incontrate nella definizione del sistema nelle variabili del modello esistente, soprattutto a causa della mancanza di dati. Pertanto, i test che sono stati condotti in scala di laboratorio sono stati provati ad essere simulati per valutare alcuni dei parametri del modello. Alla fine, è stata raggiunta una giusta approssimazione del funzionamento dell'impianto reale.

Parole chiave: digestione anaerobica; impianti di trattamento delle acque reflue; ADM1; co-digestione.

Abstract

The fate of wastewaters has always received high attention due to their harmfulness to both man and the environment. The treatment of wastewaters is a complex system made up of multiple steps, which require time and energy. Especially in developed countries, the Wastewater Treatment Plants have become important entities in the national electricity demand. Therefore, the Anaerobic Digestion process of the sludges has gained great importance. Its operation can be optimised in different ways. Among them, Anaerobic co-Digestion is very attractive because it allows to achieve three goals at the same time: exploitation of the oversized anaerobic reactors, that is reflected in both an increase in biogas production and a decrease in the specific cost of the process; improvement of the conditions of the anaerobic system, that is reflected in both increasing methane and biogas production; possible recover of wastes, as OFMSW, food wastes and dairy by-products. However, Anaerobic co-Digestion is a sensible system that should be managed adequately. Modelling is a beneficial tool to understand the biological processes that happen during anaerobic treatment, and so to improve their performance.

In this thesis, the simulation of a full-scale digester by means of the Anaerobic Digestion Model nr. 1 by the International Water Agency Task Group has been studied. The platform AQUASIM 2.0 was used to implement the simulation. The samples collected in the plant under study have been completely characterised. Many difficulties were encountered in the definition of the system into the variables of the existing model, especially because of lack of data. Therefore, also the tests that have been conducted at bench-scale were tried to be simulated to evaluate some of the parameters of the model. In the end, fair approximation of the operation of the real plant was achieved.

Key words: Anaerobic Digestion; Wastewater Treatment Plant; ADM1; codigestion.

CHAPTER 1.
INTRODUCTION

Water is a primary need for all living species. Our planet is even called the 'blue' one because water is predominant over the land. But only 0.5 per cent of the water on the Earth is available as fresh water, and it is not equally distributed. That's the reason why the 6th Sustainable Development Goal (SDG) in the 2030 Agenda states: "Ensure availability and sustainable management of water and sanitation for all".

Water is used by man for transportation, heating, cooking, industry and many other uses. So, from resource, the step to transform water into a waste is short. Untreated wastewater contains nutrients, but also numerous pathogenic microorganisms and potentially toxic compounds. For these reasons, treatment of wastewater is necessary to protect public health and the environment. Despite that, it is not yet adopted worldwide. As an example, in the SDG Report 2018, preliminary estimates suggest that 59 per cent of all domestic wastewater is safely treated but considering only 79 mostly high- and high-middle-income countries and excluding much of Africa and Asia.

The main objectives of wastewater treatment are the removal of suspended and floatable material, the treatment of biodegradable organics, and the elimination of pathogenic organisms [1]. In the last decades, the attention has been focused on the removal of constituents that may cause health effects and that are considered contaminant when discharged to the environment.

Indeed, the degree of treatment must comply with the local regulations. In Italy, the plan about urban wastewater treatment was defined in the legislative decree no. 152/99 (today it is substituted by the legislative decree no. 152/06), in compliance with the EU Water Framework Directive 91/271/CEE. In the case the treated wastewater is reused in agriculture or for civil or industrial use, the minimum standards of quality are more restricted (see the legislative decree no. 185/03 as reference).

Table 1.1 Standards for the discharge from urban wastewater treatment plants (91/271/CEE)

Parameters	Maximum concentration	Minimum percentage of reduction
BOD5 at 20 °C without nitrification	25 mg/L O_2	70-90
COD	125 mg/L O_2	75
TSS	35 mg/L (over 10.000 PE) 70 mg/L (2.000-10.000 PE)	90 (over 10.000 PE) 70 (2.000-10.000 PE)

The constituents found in liquid wastewater and sludge are removed by means of physical, chemical, or biological processes. Physical methods take advantage of external forces, as gravity or attraction between bodies. Screening, mixing, flocculation, sedimentation, flotation, filtration, and adsorption are typical physical unit processes. Chemical treatment methods involve the addition of chemicals or other chemical reactions for the removal of constituents. Precipitation, gas transfer, adsorption, and disinfection are the most common examples. In biological unit processes the removal of constituents is brought about by biological activity. These substances are converted into gases or biological cell tissue that can be further removed by physical means.

In general, physical unit processes are applied at primary treatment level; chemical and biological unit processes are referred to secondary treatment and they are used primarily for the removal of BOD5 and TSS; combinations of all three is referred to tertiary level, required in case of reuse. Advanced treatment processes are used to produce potable water.

Coarse solids are produced from raw wastewater by screening and grit removal, and they are typically sent to landfill. Primary sludge is produced from the primary sedimentation of raw wastewater, and secondary sludge is produced from the biological treatment of wastewater. These streams are mixed together and treated further, commonly with anaerobic digestion.

The stabilisation of wastewater is the main consumer of energy in the treatment facilities. Furthermore, the energy demand is increasing because the required level of sanitation and the limits of emissions have become more stringent, and the world population has increased, so the number of WWTPs. Because of that, the amount of wastewater to be treated and the efforts to do it have increased.

Longo [2] reports that in Germany and Italy electricity demand for wastewater treatment accounts for about 1% of total consumption of the country. In the case of Italy, it corresponds to about 7.5 billion kWh/year. In Spain and U.S., it is estimated that the total energy consumption of water management (not only wastewater collection and treatment, but also potabilization and distribution of water) is about 4% of the electricity demand.

For these reasons, in addition to increasing energy costs, shortage of fossil fuels supplies, and increasing awareness of the impacts of emissions in the environment, concern over the rate of

consumption of energy has increased. Water agencies and WWTP operators are becoming more interested in the achievement of efficient energy management.

On the other hand, wastewater has a great energy potential. Its organic and inorganic constituents could undergo exothermic reactions, and chemical energy is released. During the treatment processes, some of it is extracted and transformed into biomass and reaction products, as carbon dioxide and water, or released as heat through metabolism of microorganisms. Biomass can be transformed into biogas and syngas through sludge processing. However, historically WWTPs were not designed to maximize the chemical energy recovery [1].

Wastewater retains also thermal energy as its temperature changes. Heat can be extracted also from exhaust air from unit processes. It is common to utilize the excess heat for digester heating, solids drying, hot water supply, and buildings heating. If it is large enough, excess heat can also be transferred outside of the treatment plant.

Finally, hydraulic energy of wastewater fluid is usually quantified in terms of the Bernoulli equation. It is the sum of the gravitational potential energy due to elevation head, energy associated with pressure head, and kinetic energy embodied as velocity head. The hydraulic energy of the fluid can be converted to mechanical power through turbines or pumps.

Energy consumptions in WWTPs are affected by different factors. First, the size of the plant: the energy consumption decreases when increasing the population equivalent served. According to the literature, large plants are normally more energy efficient. This could be due to economy of scale, more stable operational conditions, or automation of the treatment processes. Then, energy consumption of WWTPs depends on the type of treatment and adopted technology. As expected, membrane bio-reactor systems are the most consuming ones, due to the requirement of intensive aeration rates, meanwhile conventional activated sludge and aeration pond processes consume less energy. WWTP operational indicators are usually defined as dilution factor, and load factor. The influent wastewater may be subjected to dilution due to infiltration of rainwater, so energy consumption increases when increasing the dilution factor. The inlet flowrate and loadings are also characterised by strong diurnal, weekly and seasonal variations. Because of this reason, WWTP must be oversized and the equipment must be installed with greater power than requires. As result, the capital cost is excessively increased and there can be energy inefficiencies if the plant receives lower loadings than design values. There can be also inefficiencies from the treatment point of view, leading to deteriorating effluent quality. Moreover, the impact of influent dilution and plant load factor on energy consumption decrease increasing the size of the plant.

As the WWTP is a complex system, each treatment process presents very different energy consumption rate. In conventional medium to large plants, the higher energy supply is required by biological treatment, either for aeration blowers, influent pumping or effluent recirculation; pumping systems for the transfer of any kind of flow; and generally mechanical

dewatering of sludge and/or aerobic sludge digestion. If it is feasible, anaerobic sludge digestion is more energy efficient as the biogas production may reduce the energy costs and improve the self-sufficiency of the WWTP.
Therefore, design, construction, and operation of wastewater treatment facilities is submitted to many sustainability issues, such as the overall energy balance, the release of greenhouse gases to the atmosphere, the use of chemicals, and the discharge of nutrients and trace constituents into the environment. Nevertheless, now wastewater can be considered a recoverable source of energy, resources, and water. The development of new technologies can transform wastewater treatment plants from being consumer to net exporters of heat and chemical energy. Thanks to advanced processes, also the reuse of treated and sanitized water would be possible.

1.1 Processing and treatment of sludges with AD

All constituents removed in wastewater treatment plant are described as sludges. They represent the largest flowrate, and their processing and disposition present a complex problem. Sludge is composed largely of organic matter and only a small part is solid matter, so it will decompose and become unpleasant if untreated. If properly handled and processed, sludge can be recovered and reused according to the regulations for the protection of public health and the environment.
The composition of sludge varies depending on the origin of it, its aging, and the type of processing to which the sludge has been subjected. Typically, the largest volume is composed of primary and activated sludges. Primary sludge comes from the primary settling tanks; it is usually dark, slimy and extremely malodourous; it can be readily digested. Activated sludge is usually brown, with a flocculant appearance and an inoffensive odour; it tends to become septic rapidly; it digests well aerobically. Mixed sludge is the mixture of primary sludge and waste activated sludge coming from secondary settling tanks.
Important chemical constituents of sludge are nutrients, including nitrogen, phosphorous, and potassium. Their concentrations are important in considering the ultimate disposition of the treated sludge. Together with its content of organic material, pathogens, heavy metals, and toxic organics, they affect the suitability of treated sludge as soil fertilizer or dispatch to incineration. Instead, the measurement of pH, alkalinity, and organic acid content are important control variables in the anaerobic digestion process of the sludge.
Infinite number of combinations are possible for the sludge processing flow diagrams. The most common layout involves biological treatment for the stabilization and a system to dewater the sludge. Preliminary operations, as screening or grinding, are also needed to provide a relatively constant and homogeneous feed to subsequent facilities. Thickening processes, as gravity settling and centrifugation, are performed in order to increase the solid

content of sludge, and so decrease its volume. This is beneficial also from an economic point of view, because the sizing of subsequent equipment, the quantity of required chemicals, and the amount of heat for the digesters or performing drying can be reduced.

Stabilization of the sludge is performed in most of the wastewater treatment plants to reduce pathogens, eliminate offensive odours, and limit putrefaction. Furthermore, it can result in the production of usable gas, as methane, and improved sludge dewaterability. The principal methods are alkaline stabilization, anaerobic digestion, aerobic digestion, and composting.

As already cited, anaerobic sludge digestion is a process with the advantage of both achieving a good stabilisation and being a possible net energy producer because methane is produced. As opposed to aerobic process, anaerobic digestion has energy savings by eliminating aeration, and reduced processing and disposal cost due to lower biomass production. Moreover, it generally has higher volumetric organic loading rates so that smaller reactor volumes are required for the treatment. On the other hand, anaerobic digestion requires skilled operation to maintain process stability. Due to the nature of the process, volatile fatty acids production by the acidogens and the capacity of the methanogenic organisms must be maintained in balance; that is achieved by a proper control of the feed, temperature, and pH.

Wastewater characteristics have effect on the anaerobic process design. Its operation is more stable if the feed has a uniform flowrate and organic loading. In case of wide variations, flow equalization must be considered to avoid imbalance between different microorganism populations. Stable reactor temperatures of 25 to 35°C and high biodegradable COD concentrations (1500 to 2000 mg/L) are generally preferred to obtain optimal biological reaction rates and enough methane content in the produced biogas.

If anaerobic digestion is performed at lower temperatures, reactions occur with slower rates and so longer retention times are required, that means larger reactor volumes and lower organic loadings. Instead, if the influent wastewater is diluted, there losses in the performance of the treatment and it may be necessary to operate at higher temperatures.

If influent wastewater has high solid concentration, longer retention time of the sludge in the reactor may be needed because of the slower hydrolysis step. This is the reason why some anaerobic treatment processes are divided into two phases, each of which is carried out in a proper reactor: in the first phase, the sludge undergoes hydrolysis and acid fermentation; the second phase is methanogenesis. However, solids may be reduced by gravity settling during sludge pre-treatment.

During fermentation, the concentration of dissolved carbon dioxide in the liquid phase could be high. If needed, alkalinity must be added to maintain an acceptable pH, and its purchase can affect significantly the cost of the process. Furthermore, addition of trace metals may be needed for the growth of methanogenic bacteria and so increasing the COD removal efficiency in the anaerobic process.

Finally, wastewater contains either inorganic or organic substances that may be toxic to the anaerobic process, such as certain heavy metals, chlorinated organic compounds, and high nitrogen concentration. For example, sulphate reducing bacteria compete with the methanogenic bacteria for organic compounds. High concentrations of oxidized sulphur compounds can be toxic, and hydrogen sulphide is malodorous and corrosive to metals too. Moreover, acetoclastic methanogens are sensitive to the presence of free ammonia, coming from ammonium and degraded proteins. Pre-treatment of wastewater and its proper control of temperature and pH may reduce the toxicity.

The performance of sludge treatment can be improved through different ways as already mentioned. Another possibility that has become very attractive in the last times is codigestion. It consists of treating a mixture of different types of wastes from different sources by anaerobic digestion in the same reactor. This practice may be attractive in wastewater treatment plants with excess capacity, or in facilities that needs to increase the amount of feed in reactors for economy of scale reasons. The main benefit of codigestion is the increase in methane production, and so larger availability of energy onsite. Furthermore, since the composition of the feed in the anaerobic reactor changes, addition of alkalinity and nutrients may be not necessary anymore.

The overall anaerobic digestion process involves three steps: hydrolysis, fermentation, and methanogenesis (Figure 1.1). An intermediate step, called acetogenesis, occurs for some organic acids produced during fermentation (acidogenesis). All the biochemical reactions are carried out by different microorganisms. During hydrolysis, a variety of bacteria produces extracellular enzymes that let biodegradable particulate material be converted to soluble compounds. During acidogenesis, bacteria produce organic acids, carbon dioxide, and hydrogen from sugar monomers, amino acids, and long chain fatty acids. Intermediate products, as propionate, valerate, and butyrate, are further converted during acetogenesis. In the fermentation processes, the substrate serves as both electron acceptor and donor to reach acid-base equilibrium. In the last step, methanogenesis, two different group of archea organisms are involved: acetoclastic methanogens, that produce methane from acetate, and hydrogenotrophic methanogens, that produce methane from hydrogen and carbon dioxide. Microorganisms live in a syntrophic relationship: for example, if hydrogen is produced too fast and methanogens do not utilize it, it can accumulate and so reduce the rate of fermentation, accumulating the concentration of volatile fatty acids and lowering pH in the reactor.

Kinetics in anaerobic digestion is very important because each process occurs at different velocity. The slowest steps are considered the rate-limiting ones of conversion and so COD removal, and they are the production of soluble substrates during hydrolysis and their following utilization during fermentation and methanogenesis. Hydrolysis rates can vary in a large range, depending on the composition of the feed substrate and the working temperature.

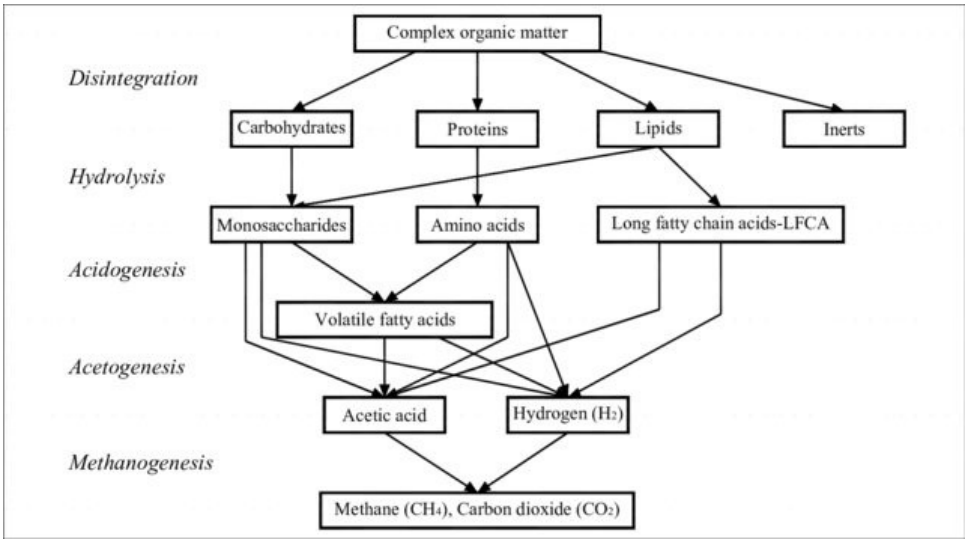

Figure 1.1 Flowchart of the simplified AD process

Long solids retention time in the reactor is required to avoid washing out the soluble substrate. On the opposite, VFAs production has faster kinetics and their accumulation can slow down the activity of methanogens, but adequate concentration of microorganisms can maintain stable conditions. Moreover, if sudden change in concentrations happen due to change in loading, populations may not adapt to it. High alkalinity can buffer the variation in pH and avoid instability, and if it is not enough, it is necessary to add it. This is the case of transient loads to the digester in codigestion.

In the implementation of anaerobic processes for sludge treatment, many design parameters must be taken into consideration. First, it must be defined the treatment efficiency that is required to meet the discharge standards. Then, the most important sizing parameters are organic loading rate, solids and hydraulic retention time. Organic loading rate is used to determine the reactor volume, and it is affected by the type of anaerobic process that is adopted, type of wastewater and working temperature. Minimum solids retention time must be determined to avoid washout of substrate. Biomass concentration in the reactor sludge increases with higher SRT. Processes at low temperature needs longer SRT because of lower reaction rates. Anyway, the removal rate efficiency is determined by both OLR and SRT. Finally, hydraulic retention time is directly related to reactor volume and influent flowrate. All design conditions must be referred to peak hydraulic loading, so that all processes can be sustained also in critical situations. Further issues that are taken into consideration are inlet flow equalization and pre-treatment, temperature control, corrosion and odour control, chemical addition, sludge and gas post-treatment.

The design parameters are used to predict reactor volume requirements, organic content of the effluent, and gas production. However, the operation of the anaerobic process has been

developed through simulation models. The most common model of anaerobic sludge digestion is ADM1, developed by an International Water Association task group.

1.2 Objectives

Generally, the potential of the AD process in the WWTPs is not completely exploited due to the unbalances of its operating conditions and the oversized design. Some methods could be applied to control the process and avoid the risk that it is arrested. Moreover, some adjustments could improve the AD process in order to enhance the biogas production. The exploitation of biogas would contribute to the sustainment of both the AD process and the energy requirements of the WTTP.

Therefore, the main objective of this thesis is the simulation of the AD process in the sludge treatment line of a real WWTP. The model would be useful to predict the biogas production in the case some changes to the operation of the plant are made, as the addition of a co-substrate. The construction of a model for complex process as anaerobic digestion consists of many steps. Thus, the model that is assumed in this thesis is taken from literature. However, the model must suit the operation of a real plant, and so additional objectives are set:

1. Complete characterisation of the inoculum and substrates of the AD reactor.
2. Implementation of the model in a validated platform.
3. Calibration of the full-scale digester model with historical data.
4. Simulation of the full-scale digester in the future operation.

In Chapter 2, a general literature review about the WWTPs is reported. In the first part, energy consumptions and sustainability of WWTPs have been investigated. Then, anaerobic codigestion is introduced as a valuable solution to recover the energy potential of sludges. Finally, modelling has been reviewed as an optimisation tool. In Chapter 3, a description of all the analytical and statistical methods adopted to perform a complete characterisation of the samples, together with the anaerobic biodegradability and activity tests, is provided. Furthermore, the AD model is described. In Chapter 4, the results of all the experiments are showed. The implementation of the AD model in the simulation platform is studied, and its outputs are reported and discussed. The calibration of the model followed the steps highlighted in Figure 1.2. In Chapter 5, final conclusions are derived from all the results that have been obtained. Possible future developments on the work established in this thesis are presented.

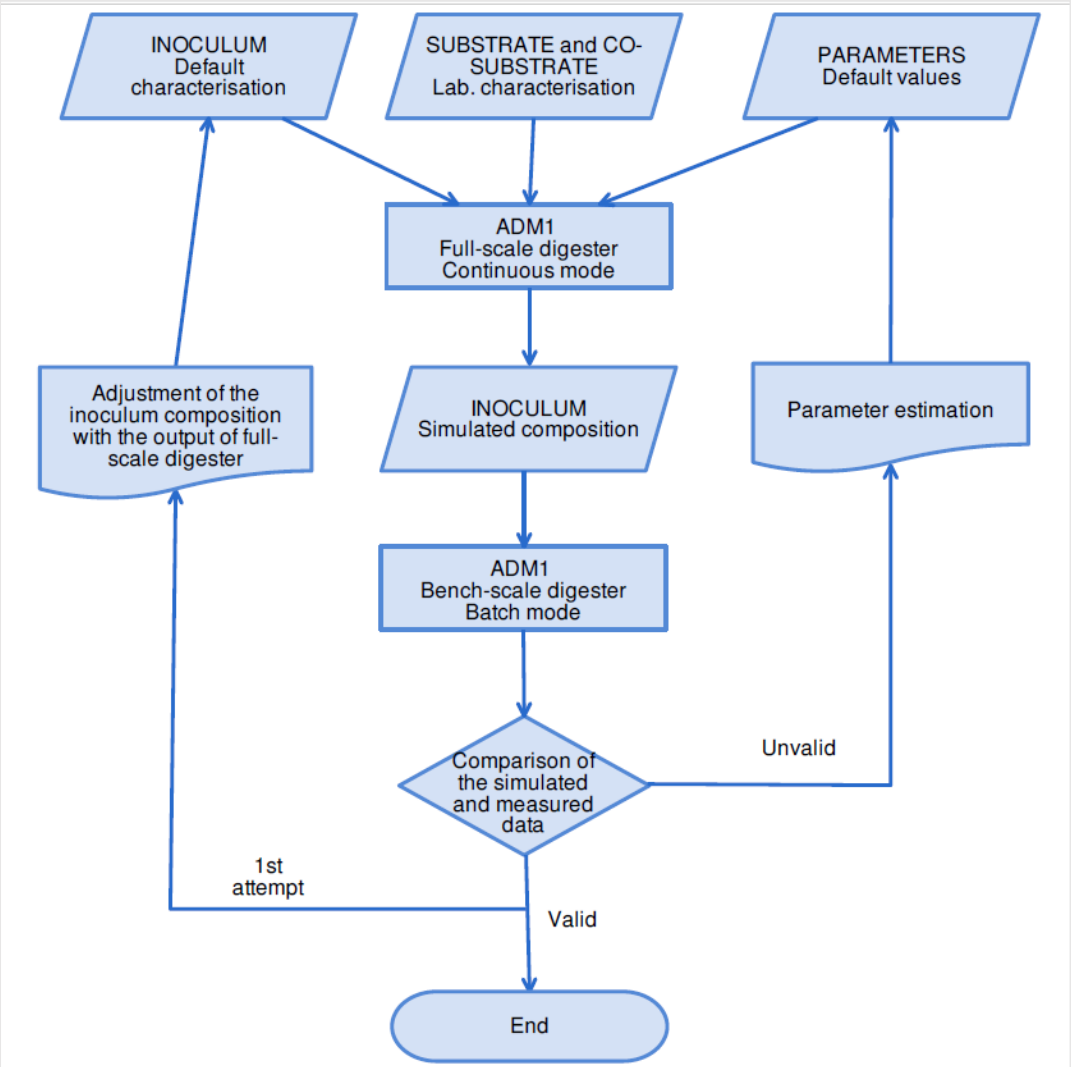

Figure 1.2 Flowchart of the steps that have been adopted to calibrate the model of the full-scale digester

CHAPTER 2.
LITERATURE REVIEW

2.1 Energy consumptions and sustainability of WWTPs

Most of WWTPs are designed to meet effluent standards. But then, the improvement of effluent quality is accompanied by the increase in energy consumption, and so increase in operational costs. Energy consumptions in a WWTP can be allocated to different sources. First, electricity requirements depend on the type of technologies that have been adopted in any treatment process: for example, in a conventional activated sludge system, aeration takes up the largest share of all electricity consumption, followed by wastewater pumping. Advanced wastewater treatment consumes relatively higher amount of energy due to nutrient removal [3]. Then, energy requirements are related to the size of the plant: larger WWTPs present higher energy efficiency than smaller ones due to economies of scale. Finally, electricity consumptions depend on the regional standards set where the plant is located. In addition, the volumes of wastewater that is treated and sludge that is discharged are increasing annually due to the growth of population. Instead, in China, despite the high density of population, energy consumption of WWTPs is lower. The reasons for that can be found in less strict discharge standards, different treatment technologies [4].

Wastewater is a great potential source of energy. This could allow the WWTP to be energy self-sufficient. Most of wastewater energy is contained in the biogas produced during the anaerobic stabilization of sludge. Biogas is mainly exploited onsite: it is converted in a CHP system to electricity and heat. Otherwise, the thermal energy from wastewater is directly extracted in heat exchangers and heating pumps. Even if it does not depend on the availability of wastewater, heat can be generated by solarthermics and photovoltaic systems installed in the plant ([4], [5]).

Further improvements towards energy self-sufficiency can be done: first, by good housekeeping and proper management of wastewater. Then, process may need some modifications and equipment may need to be renewed. Finally, value may be added to the discharge, e.g. through material, heat and kinetic energy recovery [6].

Table 2.1 Some of the solutions that have already been applied to improve the exploitation of the energy content of wastewater, and so the efficiency of the WWTP

Process/technology	Operation	Ref.
Enhanced side-stream anaerobic sludge digestion	Up-concentration of organic matter into sludge biomass (adsorption, assimilation, accumulation); high-rate anaerobic digestion: quite high sludge loading rates, short SRT and quite low HRT. Direct discharge of the digestate is not possible due to high COD content. It follows deammonification process based on anaerobic ammonia oxidation.	[7]–[9]
A-2B process	Anaerobic fixed bed reactor, and sequencing batch reactor and moving bed biofilm reactor for nitrogen removal. Higher COD conversion to methane.	[10]
Anaerobic membrane bioreactors with nutrient recovery	Good robustness under mild temperature conditions. Need of membrane-fouling control and recovery of dissolved methane in the permeate. Currently most of the approaches for nutrient recovery are not economically viable and environmentally sustainable.	[9], [10]
Microbial electrochemical systems	Direct production of electrical energy or hydrogen gas. Limited available substrate for exoelectrogens (soluble volatile acids). High cost; stability issues.	[9]
Codigestion of sewage sludge with other organic wastes	Higher OLR. Improvement of the overall C:N ratio of the feedstock. Acceleration of the rate-limiting step in AD. Increase in gas digester gas production.	[7]
Sludge pre-treatment	Thermal hydrolysis (e.g. Cambi and Exelys processes): cell destruction resulting from pressure drop. Hydromechanical screw-mill (BTA process).	[7]

The numerous alternatives can make the WWTPs become energy self-sufficient. Different indicators are used to measure the efficiency and sustainability of the WWTPs in terms of energy and resource recovery.

Further improvement and process optimisation can bring to over-production of electricity and/or heat, and it can be supplied to consumers that are in the surroundings of the plant. However, losses among the distribution net cannot be neglected. A method to assess the integration of WWTPs into local energy supply concepts was proven, too [5].

In conclusion, there are still many challenges toward designing and operating energy self-sufficient WWTPs. First, the cost of many technologies is still high, and the construction of new plants requires a great investment. The limitations to application are even more noticed in developing countries [3].

2.2 Anaerobic codigestion in WWTPs

Anaerobic codigestion is a way to produce biogas improving the properties of the feeding mixture and so of the effectiveness of the involved reactions with respect to mono-digestion. AcoD can improve the process stabilisation, nutrient balance, and so the performance of microorganisms for biogas production inside the reactor. Different parameters

are important to control the digestion process: chemical properties and particle size of the feed, operating temperature, pH, organic loading rate and hydraulic retention time.

Any type of organic substrate is composed of carbohydrates, proteins, lipids and other compounds that are inert to biochemical reactions, which concentration depend on the source. For example, food waste is rich in sugars, that are easily degraded into fatty acids and so they can cause a decrease in pH inside the reactor; nonetheless, they have a great potential in biogas production and so food waste is an attractive co-substrate. Organic wastes that are rich in proteins, such as wastewater from slaughterhouse and animal manure, have a high methane potential. However, during digestion they release ammoniacal nitrogen that provides buffering capacity but whose free ammonia form can inhibit the microorganism activity. High-fat-content substrates are used for high biogas production, but they can cause also process instability. Therefore, proper C/N ratio and nutrition balance is necessary to exploit the synergistic relationship among different substrates and avoid antagonistic effects [11].

Temperature is an essential parameter to control the growth of microorganisms and so the stability of the reactions in AD. Three temperature ranges can be distinguished: psychrophilic (25°C), mesophilic (approximately 35°C), and thermophilic (approximately 55°C). Microbes can tolerate only a minimum change in temperature; ammonia inhibition prevails at high temperatures. Although biogas production increases with the temperature, its methane content decreases because the solubility of carbon dioxide is reduced.

The pH control in the digester is as important as the temperature. Each step in the AD process requires a specific level of pH. For maximum methane yield in a single-stage process, the overall optimal pH range is 6.8-7.2 which allows to balance the metabolic activity of all microorganisms. Alternatively, the AD process is divided into two stages: first, hydrolysing and acidogenic bacteria are maintained at their favourable pH range (5.5-6.5), then the methanogenic phase is run with a pH around neutrality. Advantages of the two-stage system are the reduced lag phase and the higher VS removal efficiency.

One of the main advantages of AcoD is the adjustment of C/N ratio of the feed. Carbon and nitrogen are the main sources of nutrition for the microorganisms. C/N values that are lower than the optimal one leads to higher concentrations of ammonia; instead, greater values lead to the production of large amounts of volatile fatty acids during fermentation and a potentially insufficient buffering capacity. Cattle manure presents low C/N ratio, so it is poor in degradable organics. Lignocellulose-type substrates would supply large amounts of carbon, if only lot of it cannot be utilised by anaerobic organisms [12].

The increase of OLR by the addition of a co-substrate, is an advantage from both the technological and biological point of view. First, size and cost of the digester are reduced, and the energy for heating too. Then, higher OLR enhances different microbial species. However, loading rates beyond the optimal range could cause the accumulation of VFA and ethanol and bioprocess disruption.

Finally, HRT is another key parameter. A too long retention time leads to scarcity of nutrients, and so decay of the microorganisms. Short HRT surely reduces the size of the digester and investment costs, but it can result in the washout of the microbes.

Lab-scale experiments and modelling can be useful to evaluate the expected performance of AcoD. They allow to identify both the synergistic and antagonistic effects between the co-digested mixtures [13]. Conventional analyses include Total Solids, Volatile Solids, Chemical Oxygen Demand, Total Kjeldahl Nitrogen, Volatile Fatty Acids concentrations, pH and alkalinity. The Biochemical Methane Potential test is a useful tool to evaluate the biodegradability of the substrate in relation to a specific microbial consortium (inoculum). However, it is complex and time consuming. Various alternatives have been suggested to avoid the high costs for analyses, such as AcoD modelling. It can predict and quantify the effects of mixing different wastes into the digester, and so it can improve co-substrate selection and dosage rates. However, chemical characterisation of the codigested substrates has to be known.

AcoD with sewage sludge as main substrate is very attractive because of its low bio-methane yield and the availability spare capacity in biogas plants at WWTPs. Sewage sludge (SS) is characterized by low C/N and high alkalinity. Therefore, easily biodegradable organic substrates such as the organic fraction of the municipal solid waste and fats, oil and grease are adequate and frequent co-substrates. Recently publications have reported AcoD between SS and fruit and vegetable waste, slaughterhouse waste and glycerol. Transport cost from the source to the WWTP must be taken into account while selecting the co-substrate, too.

In the literature it is present a wide range of results concerning SS and biowaste codigestion (Table 2.2). Food waste (FW) is a valuable co-substrate because of its high biodegradability and rapid hydrolysis [14]. However, this can result in some inhibition factors like ammonia and VFAs. Excessive ammonia is produced due to the high nitrogen content, and VFAs accumulate due the rapid acidification in the AD process. Therefore, FW is frequently added to the AD process of sludges, so that the characteristics of both substrates compensate each other leading to optimal C/N. Many lab-scale experiments have been performed to evaluate the effects of AcoD.

Xie et al. [13] carried conventional BMP tests to calculate the specific methane yields of SS and FW in mono and codigestion. Intermediate analyses, such as the evaluation of soluble COD, total organic acids and pH were carried during the BMP tests to evaluate the kinetic rates. The results showed that the experimental values of biodegradability in codigestion were considerably higher than those calculated by combining the specific methane individual co-substrates during mono-digestion. It was observed that the performance of the AcoD process increases with the OLR, till an optimal value is reached. Above that, lower specific methane yields and slower hydrolysis were observed. Further tests [11] also confirmed AcoD synergistic effects by examining the VS and COD removals, and COD balance. Instead, synergistic effects

Table 2.2 Typical values of the Methane Yield from batch tests found in literature

Substrate	Characteristics	Methane yield [NmL CH4/g VS]	Reference
SS	ISR = 3	248,8	[15]
Vegetable and FW	ISR = 3	350,7	
Mixed OFMSW:SS	ISR = 3, 0.23 $g_{VS\ OFMSW}/g_{VS}$	293,0	
Mixed OFMSW:SS	ISR = 3, 2.09 $g_{VS\ OFMSW}/g_{VS}$	365,5	
SS	5.67 $kg_{VS\ added}/m^3$	246,5	[11]
FW	3.56 $kg_{VS\ added}/m^3$	575,4	
FW + SS	15.29 $kg_{VS\ added}/m^3$	684,5	
Raw sludge	ISR = 2	320,0	[16]
FW	ISR = 2	450,0	
FW:Raw Sludge	ISR = 2, 12.5 %mass	360,0	

in codigestion of SS and FW were associated with the improved kinetics in acidification and methanogenesis stages [11].

Kim et al. [17] conducted several tests in semi-continuous flow anaerobic digesters treating a mixture of FW and SS (primary sludge and thickened wasted activated sludge with different blending ratios). The results showed that the COD removals and degradation kinetics were higher during codigestion than mono-digestion. On the other hand, soluble nitrogen concentrations of digestates increased, causing drawbacks in energy consumptions for treating the reject water. Tests for controlling the microbial activity were conducted too (specific methanogenesis activity, specific acetogenic activity, and specific acidogenesis). Although it is widely assumed that the positive effects of FW are related to the increase of C/N ratio of the inlet mixture, from the results it was clear that the biodegradability of FW significantly enhanced AD.

Liu et al. [18] compared results obtained from batch AD of various substrates at low solid concentration (TS 4.8%) and high solid concentration (TS 14%). In each case, different proportions of SS and FW were adopted. In both low- and high-solids groups, biogas production was positively proportional to the content of FW in the substrate. However, the VFAs produced in the degradation step increased significantly in the low-solids groups, increasing the risk of inhibition. In the high-solids group, acidification was moderated by the high alkalinity originated from the release of ammonia, that created a weak alkaline environment in the reactor (pH 7.5-8.5). On the contrary, free ammonia could still inhibit the system. The high-solids group had better overall performance, and the maximum biogas production rate was achieved at 50% blend ratio of FW with sludge. Furthermore, some of the

authors [19] investigated if high-solids AD possibly suffer the shock of some high-concentration ingredient in substrate, such as salt in FW. The results indicated that the digestion process was significantly lower, but without accumulation of intermediate products and system instabilities.

Koch et al. [16] performed batch tests to observe changes in the specific methane yield in codigestion and assessed the best ratio between SS and FW. In general, the methane yields of the mixtures improved with increasing share of FW. However, a local maximum of the methane production was observed with a ratio of 12.5% (w/w). In order to quantify synergistic effects of the codigestion on gas production, the results from the batch tests were not suitable because the microbes usually require long time to reach steady state. Therefore, continuous experiments are necessary. Codigestion was performed at full-scale in a WWTP (10% w/w mixture of FW with raw sludge). Productivity was increased due to the co-substrate addition and enhanced rate-limiting hydrolysis. However, the methane concentration was slightly negatively influenced. The main drawback in performing codigestion was a slightly higher energy demand caused by the treatment of ammonia rich-reject water. AcoD process is followed by the exploitation of biogas in a combined heat and power unit. For the case of the WWTP under study (Garching, Germany), that treats wastewaters of approximately 30.000 PE under mesophilic conditions, it was estimated that self-sufficiency of the WWTP under study could be reached at a FW ratio of about 16% (w/w) while treating 12,000 PE.

On the contrary, Guven et al. [20] estimated the energy recovery directly from the experimental data for biogas production obtained in the lab-scale digester. The theoretical methane yield was calculated by assuming the complete degradation of the COD; therefore, the actual methane yield is always lower. So, an energy neutral or even energy positive WWTP operation could be achieved by improving organic matter capture and minimizing aeration energy demand through good management practices, together with codigestion in the anaerobic process.

Good management practices regard also transportation and storage. They may represent an important cost if the feedstock is not available in the surroundings of the WWTP. Some agro-industries by-products represent a good option as co-substrates. Indeed, Maragkaki et al. [21] performed a series of laboratory experiments adding FW, cheese whey, and olive mill wastewater (FCO) in different concentrations to the SS in the codigestion process. In order to reduce the volume of the feedstock, and so reducing its cost of transport and storage, it was mixed and dried in a thermal process. Laboratory tests were run in continuous. As expected, the daily biogas production was found to increase as the FCO concentration increased, reaching an optimal value when 5% FCO was used; 70% of methane content was achieved. A larger content of FCO revealed a higher biogas production, but a decrease in methane content. So, drying the mixture of co-substrate did not negative affect the process, actually it improved

it. It was proposed to furtherly develop the system with solar drying, so that energy consumption and drying system cost would be reduced.

Hamzawi et al. [22] evaluated the feasibility of the AcoD process of sewage sludge and OFMSW as a solution to the problems of waste management. Measurements of biogas production, methane concentration, and all the key feed properties were conducted on lab-scale batch reactors with different substrates ratios. The mixture with 25% v/v OFMSW produced the highest quantity of biogas. Further investigations revealed that alkaline pre-treatment increased the biodegradability of the AcoD mixture the most, as compared to the untreated control, thermal and thermochemical pre-treated feed.

The same proportion of the feed was assumed by Sosnowki et al. [23] for conducting digestion tests on both batch mode and quasi-continuous mode. The latter was conducted in two separated stages: acidogenic digestion under thermophilic conditions and mesophilic methane fermentation. The results from batch experiments revealed that the biogas produced from the mixture of SS and OFMSW is larger than in mono-digestion, but the kinetic of the process is slower at high rather than at low OLR. The process conducted in two-stage system was more effective than that carried out in batch mode.

Cabbai et al. [15] conducted several BMP tests at mesophilic temperature on SS together with different types of source selected OFMSW. The maximum methane yield was observed for restaurant (675 NmL CH_4/g VS) and canteens organic wastes (571 NmL CH_4/g VS). Further tests were conducted on SS co-digested with mixed wastes from different sources. The choice of the co-substrates was based on their availability near the WWTP, in order to reduce the shipping costs. The sample with 50% of OFMSW added to the supply feed highlighted an increase in methane production of 47%, compared to mono-digestion of SS. Furthermore, AcoD is the proper process to lower the inhibition risk due to the acid load of some source selected OFMSW. Based on the results of the BMP tests, pilot plant tests were carried out [24]. Different values of OLR were applied in order to find the value that maximized the production of biogas. Also, early process indicators like VFA and FOS/TAC were always monitored to control if inhibition occurred. It was observed increasing VS/TS ratio with organic loading, highlighting the OFMSW greater contribution to the mixture organic content. During the test period, the pH remained almost stable to a neutral value, while the VFA concentration in the substrate increased. This happened thanks to the increasing buffering capacity in the reactor.

Algae are another type of bio-waste that could be suitable for AcoD with wastewater sludge. It is very appealing because they can be produced within the WWTP, so the transportation costs of the feedstock would be avoided. Mahdy et al. [25] conducted a study to assess the potential of algae for AD with the other wastes generated during wastewater treatment. AD was conducted in batch mode. Substrates chemical characterization revealed that microalgae and activated sludge biomass are quite similar. Both showed also low biodegradability, so they were thermally pre-treated in order to improve hydrolysis and methane production. When

compared to the digestion of pre-treated microalgae biomass and primary sludge substrates alone, their codigestion enhanced methane yields.
Also Wang et al. [26] investigated the AcoD of algae (Chlorella) with waste activated sludge. Mesophilic digestion was performed in batch mode. The results showed an increase in biogas yields from algae during codigestion. It was proposed to recycle the released nutrients from AD of algae and sludge for additional algal growth at WWTP.

2.3 AD process modelling

Due to the complex nature of AD, mathematical modelling is a valuable tool for both simulation and control purposes. In literature, comprehensive reviews about AD modelling can be found ([27], [28]) in which the steps to follow in modelling are highlighted: first, model selection, partially driven by the amount of a priori knowledge available on the system; then, parameter selection for calibration; data collection, e.g. experimental measurements; parameter estimation, based on cost functions or objective functions; accuracy estimation; finally, the resulting model should be subjected to a validation procedure.
With regards to the parameter selection, Boe et al. [29] tested several online and offline indicators: biogas production, pH, VFAs, dissolved hydrogen, methane and hydrogen content in the biogas. Their responses to hydraulic and organic load disturbances were measured and compared. However, none of these indicators showed response to all perturbations. Thus, the combination of different indicators might be necessary to cover all imbalances situations. Furthermore, in the case of full-scale application, reliability and robustness of the online sensors should be considered.
De Gracia et al. [30] proposed a generic digester model to be easily integrated into a WWTP model (plant-wide modelling methodology). The proposed model could simulate the main biochemical transformations, and it was linked to a thermal model for simulating the temperature evolution. Finally, the model was properly calibrated using numerous experimental data both from bench-scale reactors, pilot plants and full-scale digester. All these digesters were fed with primary, secondary and/or the mixed waste sludge produced at the Tudela WWTP (Spain). The substrates were carefully characterised using the methodology for the automatic estimation of influent characteristics based on optimisation algorithms presented in a previous study [31]. The simulation of the pilot plants and full-scale digester served as validation of the model calibration.
Donoso-Bravo et al. [32] applied different mathematical models to calculate the performance parameters for batch AD, using the experimental data from BMP tests on primary and secondary sludges. The transference function, or Reaction curve-type model, was also evaluated. It considered that any process might be analysed as a system receiving inputs and generating outputs.

$$B = P\left(1 - exp\left(-\frac{R_m(t-\lambda)}{P}\right)\right)$$

Where B was the biogas produced; P maximum biogas production; R_m maximum biogas production rate; λ lag time. This model resulted more accurate in fitting the measured data points than other models. Furthermore, thermal and sonication pre-treatments were evaluated using the same models.

Since hydrolysis is often assumed to be the rate limiting step in AD, interest has been demonstrated about modelling the its kinetics. Traditionally, it has been modelled according to the first-order kinetics. As alternative, Koch and Drewes [33] applied a Monod-type model for estimating the hydrolysis constants of particulate matter by fitting the data that were collected from an anaerobic batch test with SS.

$$B = \frac{(F_0 \cdot G)k_{hyd} \cdot t}{1 + k_{hyd} \cdot t}$$

Where $Fo{\cdot}G$ was the ultimate methane yield of the substrate added. This value, however, is usually not achieved in a batch test. therefore, the authors proposed a relationship to directly calculate the hydrolysis constant from the time (t) when the daily gas production falls below 1% without the need for data fitting.

$$k_{hyd} = \frac{t - 100}{t - t^2}$$

For complex substrates, Vavilin et al. [34] used the surface-related two-phase and the Contois models to describe the hydrolysis process in AD. The two-phase kinetics considered surface colonisation and biodegradation separately; the Contois kinetics considered growth of hydrolytic/acidogenic biomass. In general, these models showed a better fit to experimental data from a wide range of organic wastes at a high or fluctuant organic loading rate. However, the first-order kinetics model is very effective at a high biomass to substrate ratio [34].

$$\frac{dS}{dt} = -k_{hyd} \cdot S$$

$$\frac{dP}{dt} = \alpha \cdot k_{hyd} \cdot S$$

Where S and P were the substrate and product of hydrolysis, respectively; α was the conversion coefficient of substrate to product.

Despite the BMP test is a very useful tool, it requires long testing times (from 20 to >100 days). The test length could be shorten by combining laboratory tests and accurate prediction algorithms for the biodegradability and the required degradation time of a substrate [35]. Mottet et al. [36] showed the link between the initial characteristics of SS and their thermophilic anaerobic biodegradability. Several partial least square models were used, and the most appropriated one was based on biochemical characterisation (carbohydrates, lipids and proteins) and two macroscopic parameters (soluble organic carbon and the ratio of

chemical oxygen demand to total organic carbon). Furthermore, Da Silva et al. [37] developed a statistically robust mathematical strategy using sensitivity functions for early prediction of the BMP first-order model parameters, e.g. methane yield and kinetic constant rate.

As already seen, codigestion is a promising method to utilize various types of organic wastes at WWTPs. AcoD systems are commonly designed on the base of the total methane production quantity as the sum of the methane conversion multiplied by the feeding quantity of each co-substrate. However, this estimation is not accurate, because it does not consider the synergistic and antagonistic effects of the influent mixture. Therefore, Hidaka et al. [38] proposed an alternative for the substrates characterization. The relationship between total and soluble elemental concentrations was correlated with the periodic table. A simple mathematical model was built with reaction rates expressed as the multiplication of a rate constant and a microorganism concentration, effect of ammonia as a half saturation inhibition constant, and the time course was calculated using the Runge-Kutta-Gill method. The results showed successfully application of the model to both batch and continuous experiments under mesophilic conditions.

Kiely et al. [39] reported the results from a bench-scale laboratory experiment on the codigestion of OFMSW and primary sewage sludge, and they were used to develop and validate a two-stage mathematical model of acidogenesis and methanogenesis. Moreover, the model considered the ammonia inhibition and included the computation of pH. The results of the model were satisfactory for simulating pH, ammonia, and methane production. Thus, it proved the potential of AcoD to enhance biogas productivity.

Several models have been created to adjust the blending ratio between the different co-substrates, too. Garcìa-Gen et al. ([40]) proposed, and then validated, a linear programming optimisation model aiming at maximising COD conversion into methane, but simultaneously maintaining a digestate and biogas quality. The model was based on conventional substrates characterisation and BMP tests.

The International Water Association group has developed a generic model for the process of AD. Many benefits can be derived from it [41]: further development work on process optimisation and control, aimed at direct implementation in full-scale plants; common basis for further model development and validation studies to make outcomes more comparable and compatible; assisting technology transfer from research to industry.

2.4 Anaerobic Digestion Model nr. 1

The ADM1 model has been widely applied to simulate the digestion process of different substrates, bringing about suitable updates and extensions. In ADM1, the conversion processes that occur during AD are divided into two main types.

1. Biochemical: these processes are normally catalysed by enzymes and they act on the pool of available organic matter (COD, inorganic carbon and inorganic nitrogen). The model includes a partially extracellular disintegration step of composite (such as fresh content from the substrate and dead biomass) to particulate constituents and an extracellular hydrolysis step to soluble monomers as well as intracellular growth and decay of the biomass. In the growth process, they are distinguished three overall steps: acidogenesis, acetogenesis and methanogenesis. All the steps include parallel reactions in turn.
2. Physico-chemical: these processes are not biologically mediated. They involve ion association/dissociation in the liquid phase and gas-liquid transfer. Solids precipitation is not included in the ADM1.

A Petersen matrix is used to describe all the biochemical rate coefficients and kinetic rate equations for soluble and particulates components (Appendix A, [41]). For each component (24 variables), the mass balance within a system boundary can be expressed as follows:

$$Accumulation = Input - Output + Reaction$$

The overall volume-specific reaction term for each component can be formulated by summing the products of the stoichiometric coefficients and process rates. One of the advantages of the matrix presentation method is that the conversion of COD can be easily checked. In many cases, inorganic carbon and inorganic nitrogen components acted as source or sink terms to close the carbon and nitrogen mass balances respectively. Sulphur compounds are not included in the ADM1. The carbon and nitrogen contents and yields from composites are highly variable and should be adjusted for the specific benchmark implementation [42]. All the extracellular steps are assumed to be first order. The uptake processes are based on substrate-related Monod kinetics, and they include the biomass growth processes. Biomass decay is assumed to be first order, too.

The input in the biochemical conversion process is the sludge charge entering the anaerobic digester, together with a co-substrate if it is the case. It is assumed to be composed of particulate composites (homogeneous), carbohydrates, proteins and lipids. Moreover, a considerable fraction of the input substrate is already considered as inert, so it could not undergo the biochemical processes. Additional soluble and particulate inert material is produced in the disintegration process. Then, the degradable particulate substrate is subjected to hydrolysis. The process is catalysed by the organisms growing on the particle surface. Acidogenesis is the anaerobic fermentation process that produces acids from soluble sugars and amino acids. Glucose is used as the model monomer in the ADM1. The amino acid mixture depends on the source protein, so the stoichiometric yields of products could be predicted. The produced acids are acetate, propionate, butyrate and valerate. A small fraction of fermentation products is hydrogen and formate. Lactate, ethanol, aromatic carboxylic acids were not included in the ADM1. The organic acids deriving from hydrolysis and acidogenesis are

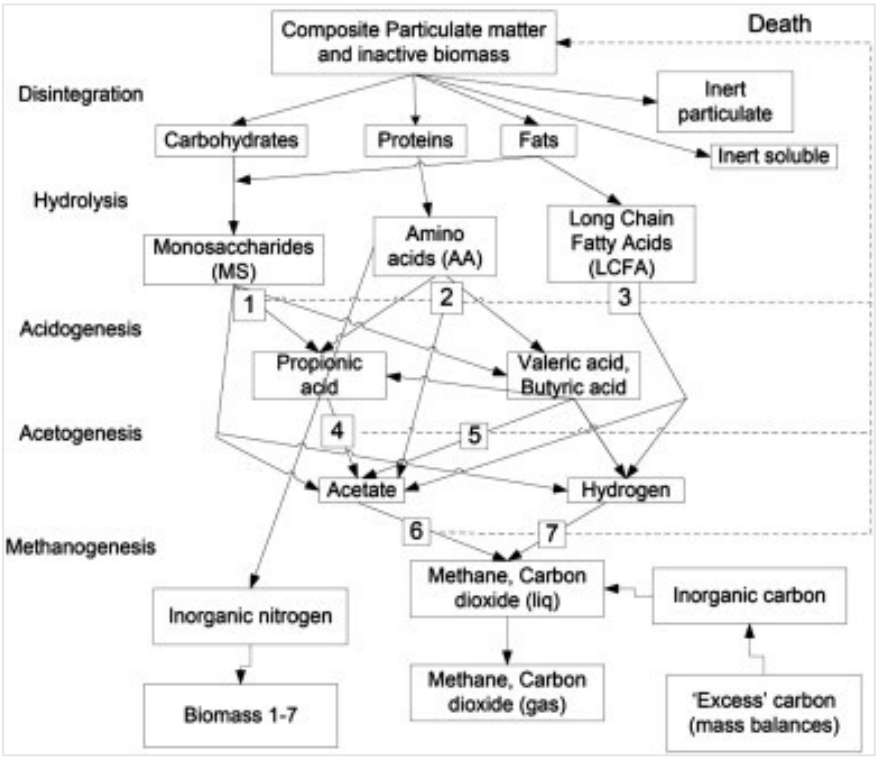

Figure 2.1 Flowchart of a detailed AD process

furtherly degraded to acetate in an oxidation step. The oxidising bacteria produce hydrogen and formate $HCOO^-$ (acetogenesis), which are consumed by archaea (methanogenesis). Three acetogenic bacterial groups were proposed in the ADM1: one for propionate, one for butyrate and valerate and one for LCFA. A single group is included for hydrogen-utilising methanogenesis. The organisms that sustain these syntrophic interactions are very sensible to hydrogen and formate concentrations, so their operating range is very narrow. This determine the parameter for hydrogen inhibition. However, the major methanogenic step consists of the cleavage of acetate to form methane and carbon dioxide. A single group of acetoclastic methanogens is used. In addition, denitrifying bacteria can grow by fermentation. These microbes reduce NO3- to nitrogen oxides, competing with methanogens for both acetate and hydrogen. Due to the complexity of the interaction between the microbial groups, nitrate reduction is excluded from the ADM1. In the end, all the anaerobic microorganisms undergo a decay process, and the dead biomass is recycled to composite organic material.

Several mechanisms of inhibition are considered (Appendix A). pH inhibition is a combination of weak acids or weak bases inhibition at low pH or high pH respectively. It affects all the organisms in intracellular processes, with different parameters for acetogens and acidogens, hydrogen-utilising methanogens and acetoclastic methanogens. Hydrogen inhibition of acetogenic bacteria and free ammonia inhibition of acetoclastic methanogens are also included in the ADM1, both described using non-competitive functions. LCFA inhibition is excluded.

For completeness of the model, secondary substrate Monod kinetics is used to describe decrease in growth when nitrogen is limited.

Temperature can affect biochemical reactions, as predicted on kinetic rates by the Arrhenius equation. In AD, there three major operating ranges: psychrophilic (4-15 °C), mesophilic (20-40 °C), and thermophilic (45-70 °C). If the temperature increases above the optimum, the reaction rates drop to zero fast. However, in the ADM1 separate values for each temperature range are used in the description of the influence of temperature instead of continuous functions. Temperature can also affect reaction pathways. Homoacetogenesis and acetate oxidation are particularly affected at psychrophilic and thermophilic temperatures respectively. However, the task group has not included homoacetogenic bacteria into the model because it is considered that most of the hydrogen and acetate are converted directly to methane.

The physico-chemical system is very important while modelling AD. It describes the major performance variables such as gas flow and alkalinity, and many biological inhibition factors such as pH and concentrations of soluble gases in the liquid phase.

All the compounds that have pK_a values (dissociation coefficients, calculated as the $-\log_{10}$ of the corresponding K_a parameter) close to the operating pH of anaerobic processes are included in the system that model acid-base reactions. The association/dissociation processes are considered as equilibrium processes since their kinetic is faster than other processes. Indeed, they can be represented by a differential-algebraic set of equations (Appendix A). The set includes the charge balance, in terms of molar concentrations, which must be always satisfied in order to evaluate the concentration of H^+ ions. An additional variable is used to represent the net charge of inert metallic ions such as Na^+ and Cl^-. LCFAs and amino acid acid-base reactions are not included in the ADM1. Since the CO_2/HCO_3^- and NH_4^+/NH_3 acid-base reactions are implemented as differential equations, the free forms are implemented as dynamic state variables in addition to the respective total forms. The equilibrium equations that describes the correlation between free and total forms are added to the set.

Three main gas components affect the biological processes or outputs: hydrogen, methane and carbon dioxide. Hydrogen sulphide and ammonia are not considered in the ADM1. There is no advective influent in the gas phase. The liquid-gas transfer is governed by Henry's law, which describes the equilibrium relationship between the phases when in contact. Despite this, dynamic gas transfer equations are used in the ADM1 because the liquid-gas transfer is related to the effluent organics and total COD balance (Appendix A). Because transfer of gases is liquid film controlled, and the diffusivities are similar, the task group suggested to use the same mass transfer coefficients for all the three kinetic rate equations. Temperature can highly affect physico-chemical reactions. Therefore, the van't Hoff equation was has been used in the ADM1 to describe the variation of equilibria coefficients with temperature. The van't Hoff formula was directly integrated in the kinetic rate equations.

2.4.1 ADM1 limitations

The original model lacks a detailed procedure for characterising the input state variable set and biodegradability. Therefore, values from literature were either assumed (mostly according to the approach described in Rosen and Jeppsson [42]) or new methodology were defined and validated. Some authors agreed that the composition of the liquid phase in the anaerobic digester could be properly adjusted by simulating the whole process, with the proper operating and feeding conditions, for an interval of time equal to 3 HRT at least. According to that, In the simulation and modelling of the mesophilic anaerobic digesting of mixed sludge by ADM1, Aboulfotoh [43] modelled the mesophilic anaerobic digesting of mixed sludge by ADM1. The author took as starting point an average feed composition of mixed sludge and the default parameters given by Rosén and Jeppsson. The simulation was run for several HRTs. Hence, the output composition of the sludge was used as initial condition of the anaerobic digester in another simulation. The model was able to predict the effluent COD, sCOD, VFAs and pH with considerable accuracy. On the other hand, the actual gas production was lower than the predicted values by the ADM1, probably due to the short time of the experiment and a leakage in the collected gas.

Astals et al. [44] proved a methodology to calculate the biodegradable fraction, the composite concentration, stoichiometric coefficients and soluble compounds of sewage sludge, based on its characterisation before and after the BMP test. The biodegradability of SS was evaluated taking into account also the amount of COD for bacterial growth and maintenance. No statistically significant relationship between the disintegration constant and the SS characterisation was found. The methodology to determine the composite concentration and stoichiometric coefficients was based on COD balances, theoretical oxygen demand and mass conversion parameters. Those values were calculated by means of elemental composition and SS characterisation results in turn. The stoichiometric coefficients of the composite biodegradable fraction presented a high variability within the SS that were studied. Nevertheless, the biodegradable fraction was close to the default ADM1 value (0.53-0.62 and 0.65 respectively).

De Gracia et al. [45] extended the ADM1 model defining the components via elemental mass fractions and estimating the COD as a function of the redox equations associated with these elements. Thanks to this approach, all the stoichiometric coefficients could be automatically calculated, and the mass and charge conservation checked. The application of this model would make the detection of possible imbalances easier and it would enable the future connection with other unit-process models. Then, Huete et al. [46] applied a similar methodology to a pilot-scale reactor treating mixed sludge. However, the model predictions of the biogas composition and alkalinity were not accurate enough. These limitations show the convenience of including the elemental characterisation of the process in terms of carbon.

In literature, several approaches can be found that utilize anaerobic respirometric analyses to estimate or calibrate the biochemical and kinetic parameters of ADM1 ([47]–[50]). In most of the cases, the resulting models showed good prediction of methane production, biogas composition, ammonia and alkalinity.

CHAPTER 3.
MATERIALS AND METHODS

3.1 Samples origin

The WWTP under study is located in the city of Sesto San Giovanni (Milan) and it is run by CAP (Consorzio Acque Potabili). In the plant the municipal and industrial wastewaters coming from the surroundings of the same city are treated, and it serves 124.500 PE with an inflow of 24.135 m^3/day. It is located next to the river Lambro, where the purified effluent is discharged. The plant scheme includes a water treatment line and a sludge treatment line. Water pre-treatments consist of screening, dragging, grit removal and primary sedimentation. After that, there are two different biological treatment lines. Part of the flow is sent to the moving bed biofilm reactor (MBBR) process, while most of the flow is sent to the biofilter process. The sludge that is extracted from the primary sedimentation undergoes another process of screening, thickening (HRT 2-3 days), anaerobic digestion (HRT 30 days) and dewatering. In the plant, there are two anaerobic digesters that operate in parallel. The biogas is extracted from the head space of each digester, and it is stored in a gasometer. Then, it is exploited in a Combined Heat-and-Power (CHP) unit for cogeneration. The unit is composed by two microturbines (65 kWel each) and a heat recovery system in the flue gases line (256 kWth). Before entering the unit, the biogas is treated, dehumidified and compressed to 4.8 bar. The thermal energy is used for heating the digesters and maintain their internal temperature around 35°C. If the temperature of the liquid phase in the digesters drops under the optimal range, the biogas is directly sent to the thermal station to sustain the heating of the reactor. If it is the case, the excess biogas is burnt off in the flare stack.
Furthermore, in the last year the plant has been revamped and two processes have been added. In the first case, organic material is recovered from dairy products that cannot be sold on the market. The raw material is treated so that the content is separated from its package, and then it is added to the thickener and sent to anaerobic digestion. In the second case, the pre-thickened sludge undergoes a rapid process of fermentation (3-5 days at 30°C). Then, the carbon-rich liquid phase is sent back to the biological treatment line to favour the denitrification process, and the solid phase is sent to the anaerobic digester.
The samples of mixed sewage sludge were collected at the entrance and the exit of the pre-thickener. The digestate sludge was sampled at the exit of the anaerobic digesters. Samples of the co-digested matrix were collected before its treatment; they consist mostly of different kinds of yogurt (fruit, fibre-rich, probiotic) that have been stored at ambient temperature in

the WWTP before being added to the process. The samples were collected in April and October 2019. After being transported to the laboratory, they were stored at 4°C. All the analyses were conducted in the laboratory A. Rozzi in Cremona.

Figure 3.1 Satellite view of the WWTP under study

Figure 3.2 The WWTP under study: on the left, the pre-thickening unit; on the right, one of the anaerobic reactors

3.2 Conventional analyses

Total and volatile solids were determined in duplicate according to Standard Methods 2540 (APHA, 2005). A fixed amount of each sample was added to an aluminium cap that was previously weighted (tare, T) and its weight was recorded (M_0). All the caps were put into an oven at 105°C for about 24 hours. After, the caps were again cooled down to ambient temperature in a dessicator and their weight was recorded (M_{105}). Then, the caps were put in a muffle at 550°C for 2 hours, plus 40 minutes that the muffle takes to warm up. After cooling in a dessicator, the final weight of each sample was recorded (M_{550}). According to the described steps, TS and VS content were calculated as:

$$TS = \frac{M_{105} - T}{M_0 - T} \cdot 1000$$

$$VS = \frac{M_{550} - M_{105}}{M_0 - T} \cdot 1000$$

The pH was directly measured in liquid samples by means of portable multi-probe meter (Hach-Lange, HQ40D).

Total chemical oxygen demand (tCOD) was determined according to Standard Methods 5220 (APHA, 2005). The method consists in the oxidation of the organic compounds in an aqueous sample using a concentrated solution of Potassium Dichromate ($K_2Cr_2O_7$ 2N) in the presence of concentrated Sulfuric Acid (H_2SO_4) and Silver Sulfate (Ag_2SO_4) as catalyst of the oxidation reaction. The excess dichromate is titrated with a solution of Ammonia and Iron (II) Sulfate. The concentration of the organic matter that can be oxidized is proportional to the amount of consumed $K_2Cr_2O_7$. In order to calculate the COD of each sample the volume of ammonia and iron sulfate required to titrate a blank (V_b), the volume of ammonia and iron sulfate required to titrate the samples (V_{AIS}), the weight of each sample (W_{sample}) and the normality of the sulfate ($N_{sulfate}$) must be known. The blank contains Potassium Dichromate, concentrated Sulfuric Acid and Silver Sulfate. Using this information, the COD is calculated as:

$$COD = \frac{(V_b - V_{AIS}) * 8000}{W_{sample}} * N_{sulfate}$$

The Total Kjeldahl Nitrogen was measured according to the ISO 5663-1984. The Kjeldahl method is a wet oxidation using concentrated Sulfuric Acid (H2SO4).

Total alkalinity (corresponding to TAC in German) was measured by means of the FOS/TAC instrument (Hach Lange BIOGAS Tritation Manager). Samples were always diluted 1:10 (10 mL of sample as received and 90 mL of deionized water). Then, they were automatically titrated with Sulfuric acid (H_2SO_4) to pH 8.3 first, pH 4.3 then. Total alkalinity was calculated as the product of the volume of acid used to reach the pH end point, the normality of the acid and the conversion coefficient of Calcium carbonate ($CaCO_3$) to equivalent (50 mg$CaCO_3$/eq), divided by the volume of the sample.

A similar instrument (Hach Lange) was used in another laboratory (located in Peschiera Borromeo and owned by CAP to run all the required analysis to monitor the WWTP under study) to measure the ratio FOS/TAC (translated to VFA/Total Alkalinity in English). Samples were automatically titrated with Sulfuric acid (H_2SO_4) to pH 5.0 to determine TAC, and from pH 5.0 to pH 4.3 to determine FOS.

Instead, in the laboratory A. Rozzi in Cremona, the VFA (acetic, propionic, butyric, iso-butyric, valeric, iso-valeric and caproic acids) concentrations were determined according to Standard Methods 5560 (APHA, 2001), using a gas chromatograph (DANI Master GC) coupled with a flame ionization detector. A Nukol fused silica capillary column was used for the separation with nitrogen as the carrier gas. A standard mixture containing 1 g/L of target acids, was used to calibrate the chromatograph. The injector and detector temperatures were at 250 °C and 300 °C respectively, and the oven temperature was gradually increased from 100 °C to 190 °C at the rate of 10 °C/min. The effluent from the column is mixed with hydrogen and air and ignited. Organic compounds burning in the flame produce ions and electrons which can conduct electricity through the flame. A large electrical potential is applied at the burner tip, and a collector electrode is located above the flame. The current resulting from the pyrolysis of any organic compounds is measured and converted into mass of the corresponding VFA. Additional measurements on the total content of VFAs in the samples (expressed as equivalent concentration of acetate) were done with the test kit LCK 365 by Hach-Lange.

Ammoniacal nitrogen (NH4+), nitrate (NO3-), total soluble nitrogen (sN) and soluble COD (sCOD) were measured using spectrophotometric test kits (Hach-Lange) on the liquid fraction of the samples after filtration on 0.45 μm filters. The test kits were chosen according to their range of concentrations and the required dilution of the samples: LCK 303 for ammoniacal nitrogen; LCK 339/340 for nitrate; LCK 338 for sN; LCK 314-514 for sCOD. The spectrophotometer used was DR6000 UV-VIS with RFID technology by Hach-Lange.

3.3 Lipids, proteins and carbohydrates analyses

Carbohydrates, proteins and lipids content must be evaluated in order to comply with the ADM1.

The lipids content (LI) was measured in both the filtered (0.45 μm) supernatant and in the centrate after centrifugation at 3000 rpm for 15 minutes according to Standard Methods 5520-B and 5520-E (APHA, 2005).

The Bicinchoninic Acid method (BCA) was selected for determining the protein content (PT) since it has an improved sensitivity and tolerance to interfering compounds compared to the Lowry method. The soluble fraction was obtained after filtering on 0.45 μm cellulose acetate filters. Appropriate dilutions of the samples were done with deionized water to fall within the calibration range of the BCA standard protocol (0-2000 mg/L). Then, 0.1 mL of standard or

sample were added to 2 mL of BCA working reagent of the Pierce BCA Protein Assay Kit by Thermo Scientific. Samples were incubated at 37°C for 30 min. After cooling at room temperature, the samples were measured spectrophotometrically at 562 nm. Bovine Serum Albumine (BSA) was used as standard for doing the calibration curve. Soluble COD and total soluble nitrogen of the BSA standard were additionally measured by Hach-Lange kit tests (LCK 514 and 338, respectively) for further conversion of the unit of measurement.

The carbohydrates content (CH) was measured by means of Dubois method on both the soluble and the total fractions. The soluble fraction was obtained using 0.45 μm cellulose acetate filters. Appropriate dilutions of the samples were done with deionized water to fall within the calibration range (0-200 mg/L). Then, 0.75 of sample was added to 0.75 mL of 5% Phenol and 3.75 mL of Sulfuric Acid (96%). After 10 min of exothermic reaction, samples were treated by vortex and left 30 min at room temperature. Then, the samples were measured spectrophotometrically at 490 nm. The calibration curve was previously done using glucose as standard.

The main issue was the investigation of the most appropriate method to induce hydrolysis on the samples, so that the enclosed PT and CH content into the molecules could be detected, too.

3.4 Hydrolysis techniques

The most accurate method to extract the total content of CH was investigated. Some methods were slightly modified from literature, and they were applied on each sample. Then, the Dubois method was used to measure CH.

1. Sample AR properly diluted with deionized water, assuming the reagents added while applying the Dubois method are enough for hydrolysis.
2. Sample AR hydrolysed as in the procedure to measure TKN, so it is diluted 1:5 with H_2SO_4.
3. Modified method described by Ohemeneg-Ntiamoah and Datta [6]: 100 mg of each sample was carefully measured, to which 3.15 mL of HCl 2.4 N was added. Following this, the sample was digested at 100 °C using a heating block for 30 min. After digestion, it was cooled to room temperature and neutralized with sodium carbonate until effervescence ceased. The volume of each sample was then made up with deionized water to obtain the required dilution for the calibration range of the Dubois method.
4. Modified method described by Lesteur et al. [7]: total sugars were extracted after 1 hour of sonication in deionized water (sample-to-mixture ratio was assumed to be 1:2 in the present study). Then, the samples were furtherly diluted with deionized water in order to respect the calibration range. In literature, this method was applied to

obtain the soluble sugars. In the present study, it was investigated if it is suitable to measure also the total content.

5. Modified method described by Lesteur et al. [7]: total sugars were extracted after 1 hour of sonication in sulphuric acid 72% (sample-to-mixture ratio was assumed to be 1:2 in the present study). Then, the samples were furtherly diluted with deionized water in order to fall within the calibration range.

All methods were tested using cellulose as the standard CH. Moreover, to evaluate if the complex matrix of the sludge matrix could contain interfering substances, the sludge samples were spiked with known concentrations of glucose as standard, and percentage of recovery was determined. In the end, the reproducibility of the method that was considered the most appropriate was verified over the samples of wastewater sludge, digestate and dairy product.

3.5 Anaerobic biodegradability and activity tests

These tests were conducted in laboratory with the Automatic Methane Potential Test System (AMPTS) II by Bioprocess Control AB. This system was preferred to manometric tests because it reduces manual handling and provides accurate and reliable data on methane gas production. The system is composed of three units: the sample incubation unit, the carbon dioxide absorption unit, and the flow cell array and data acquisition unit. The first unit consists of a thermostatic bath at 35 °C in which up to 15 reactors are immersed. Each reactor is a 600 mL glass bottle with an agitation system that is controlled in remote (rotating speed range: 10-200 rpm). The reactor volume can be filled up to 80% with the sample, so that there is some room for the produced gases in the headspace. The excess gases from the headspace is transferred to the second unit. It consists of 15 bottles (one for each reactor in the first unit) that contain an absorption liquid, NaOH 3M. The carbon dioxide in the gases reacts with the liquid solution and it is trapped as sodium carbonate. Instead, the clean flow of methane is transferred in the measuring unit. The working principle is based on liquid displacement and buoyancy of the cell at any time that 9 mL flow is transferred from the corresponding absorption bottle (measuring precision: CV ≤ 1%). The data about real-time gas flow and volume are automatically reported as standard conditions (0 °C, 1 bar) and uploaded to the specific software. The tests lasted till the time in which it was verified that the amount of methane produced in the last 3 days was less than 1% than the total cumulative production. All the experiments were conducted in duplicate. Therefore, the results could be retained reliable according to UNI/TS 11703:2018.

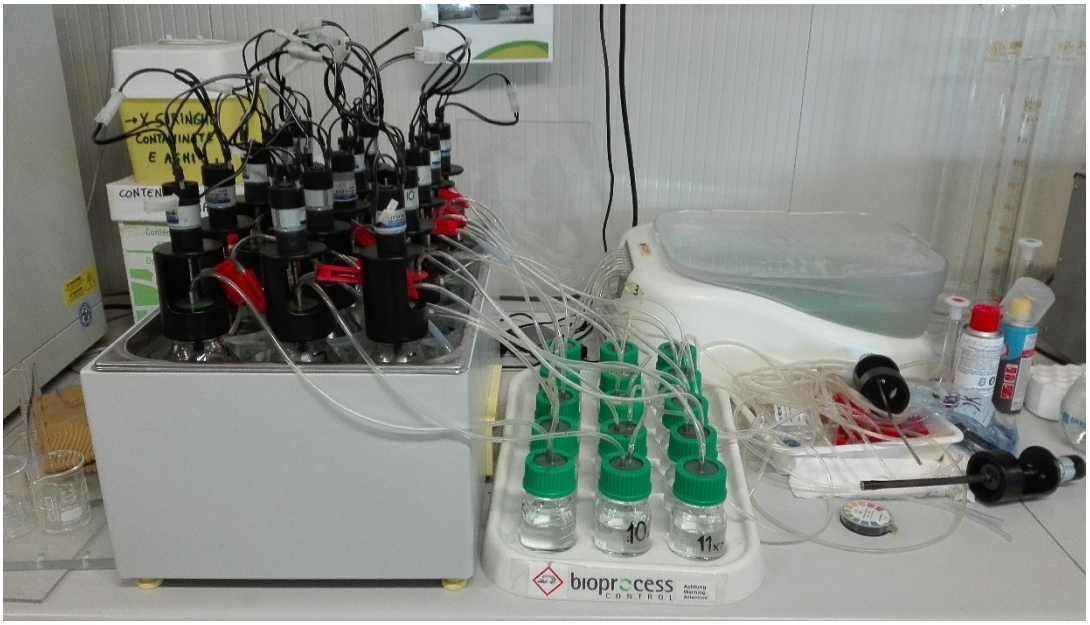

Figure 3.3 Set-up of the experiments run with the system AMPTS II; on the left, the thermostatic bath; in the middle, the absorption unit; on the right at the back, the measuring unit

3.5.1 Specific Methanogenic Activity test

In this study, SMA test was conducted on the basis of the experiments conducted by Astals et al. [9] to determine the inhibition potential of a compound. The inoculum was digestate sludge collected in the WWTP in Sesto San Giovanni. Sodium acetate ($CH_3COOHNa$) was selected as substrate. Test were conducted in duplicate. Each AMPTS II bottle was filled with 470 g of inoculum and 9.60 mL of solution of sodium acetate (100 g/L), so the ratio inoculum-to-substrate (ISR) was equal to 5 $g_{SV,inoculum}/g_{acetate}$ as suggested in the literature. Initial pH was recorded, and neither dilution water nor buffering NaHCO3 were added to the sample in the beginning. Then, the bottles were flushed with nitrogen gas and put in the thermostatic bath. The test lasted till the time that the produced biogas was less than 1% the maximum production. Data were recorded each 15 min. At the end, pH was measured again.

3.5.2 Biochemical Methane Potential test

The BMP test is the most reliable method to determine the methane yield (B_0) of a substrate:

$$B_0 = \frac{maximum\ cumulative\ methane\ (mL)}{g\ VS}$$

The first-order kinetic model is the most widely used to describe the methane production in the test ([33], [37]):

$$B = B_0 \cdot (1 - \exp(-k \cdot t))$$

Since that, the kinetic rate coefficient *k* of the rate limiting step can be derived [32]. In the case of solid waste, as SS, the disintegration of the composite material is the limiting reaction that governs the overall process.

Digestate coming from the WWTP in Sesto San Giovanni was used in all the BMP tests as inoculum. If needed, the sample of digestate was left in a thermostatic environment (35-37 °C) for some days before the experiments to reduce the specific methane production rate. First, BMP tests were conducted to check the biodegradability of the inoculum in response to the addition to different substrates. The inoculum-to-substrate ratio was suggested to fall in the range 1-4 $g_{VS,inoculum}/g_{VS,substrate}$, inoculum SV concentration in the range 5-10 g_{VS}/L, substrate SV concentration in the range 1-5 g_{VS}/L. The tests were conducted in duplicate, and blank assays containing only inoculum and dilution water were used to measure the endogenous production of methane by the inoculum. Nutrients could be added to the inoculum (composition in Appendix B). In the beginning of each experiment, the pH of each sample was measured and $NaHCO_3$ was added if additional buffering capacity was required. Then, the bottles were flushed with nitrogen gas and put in the thermostatic bath. At the end of the experiment, pH was measured again.

A BMP test was conducted with cellulose as substrate. Each bottle was filled with 400 g of inoculum, 1.4 g of cellulose and 78 g of dilution water, so that a ISR value was 3 $g_{VS,inoculum}/g_{VS,substrate}$. Another test was conducted with glucose as substrate. Each bottle was filled with 468 g of inoculum and 12 mL of solution of glucose (100 mg/L), such that ISR value equal to 2.5 $g_{VS,inoculum}/g_{VS,substrate}$ was achieved.

The biodegradability of the co-substrate that is used in the WWTP in Sesto San Giovanni was tested, too. Due to its unknown composition, an early prediction of the COD content was calculated from the average values reported in the nutritional tables on the labels of a set of dairy products. Each bottle was filled with 350 g of inoculum, 4.64 g of substrate, 52.8 mL of mixture of nutrients and 72.56 mL of dilution water. ISR value was estimated to be equal to 2.5 g_{VS}/g_{VS}. Another experiment on the co-substrate was conducted. The settings of the BMP test were adjusted according to the results of the previous one. So, the ISR was set to 3.5 g_{VS}/g_{VS} and the amount of inoculum was reduced. Each bottle was filled with 310 g of inoculum, 5.28 g of substrate, 52.8 mL of mixture of nutrients and 112.98 mL of dilution water.

Finally, a BMP test was conducted on the mixed sludge that enters the anaerobic digesters in the real WWTP. Each bottle was filled with 310 g of inoculum, 87.19 g of substrate, 52.8 mL of mixture of nutrients and 30.01 mL of dilution water. ISR value was estimated to be equal to 2 g_{VS}/g_{VS}.

3.6 Implementation of the ADM1

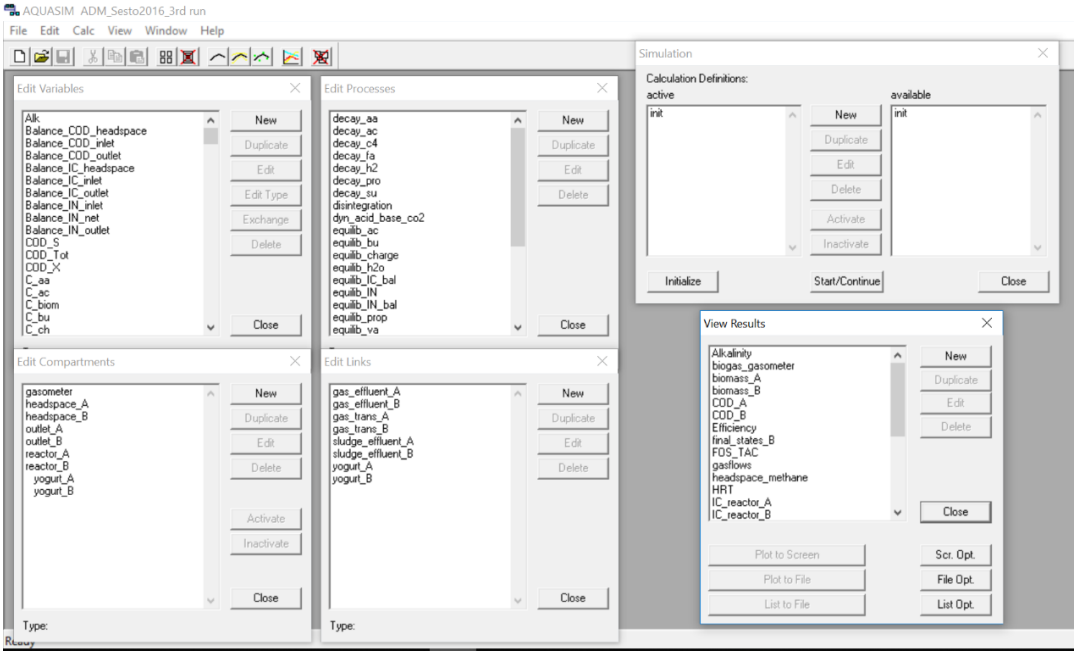

Figure 3.4 User interface of the AQUASIM 2.0 platform

The whole described system was implemented in AQUASIM 2.0. It is a computer program developed for the identification and simulation of aquatic systems by Eawag -Swiss Federal Institute of Aquatic Science and Technology. AQUASIM 2.0 allowed to describe each variable involved in the system as either state, program, constant, real list, variable list, formula, or probe variable. The state variables were distinguished in dynamic and equilibrium ones, according to the model. Furthermore, in AQUASIM 2.0 all the processes can be described. They are distinguished into dynamic processes and equilibrium ones. In the first case, they are edited the rate of the reaction and the stoichiometric coefficient of each involved variable. In the other case, the program requires the equilibrium equation to be entered as well as the variable that should be derived from that. The spatial configuration of the system can be represented as a set of compartments, in which the variables and processes that could be selected are active. The volume of the compartments can be set to be constant, so that the water outflow is equal to the water inflow, or variable, defining the quantity of the outflow. The water inflow can be defined in the input settings as either fixed or variable. In the latter case, it is defined day by day in an array. In the input settings, the loading of each variable is defined too. Advective links can be used to simulate substance transport between reactors in the same phase (liquid-liquid, gas-gas). When needed, bifurcation can be described in the advective link. Diffusive links can be used to simulate the liquid-gas transfers, according to the exchange coefficient and the conversion factor of each involved variable.

According to that, the anaerobic system was described in AQUASIM 2.0 as similar as possible to the WWTP under study. Therefore, two anaerobic digesters in parallel (A and B) were considered. The pre-thickener was not included in the simulation in AQUASIM 2.0. Thus, the sludge coming from it was described as input flow in each reactor. It was assumed that the characteristics of the influent wastewater were constant during all the time interval of simulation. An artificial compartment was added at the entrance of each digester, connected by an advective link, in order to simulate the loading of the co-substrate. For this reason, it was assumed that the characteristics of the mixed substrate would not change in the pre-thickener. The liquid and gas phases in the anaerobic reactors were considered as separated mixed compartments ("reactor" and "headspace") because they involve variables and processes of different nature. The gas flows produced in the headspaces were collected in a gasometer. The gasometer was considered as a constant volume reactor. Thus, the biogas, which amount is the same as the biogas that is instantly produced, is extracted and used either in the CHP unit or in the thermal station. This complied with the gasometer operation that was illustrated by the operator of the plant. The composition of the digestate and of the gases that were already present in the anaerobic reactor and in the headspace respectively, could be defined in the initial conditions of each compartment.

The system in AQUASIM 2.0 was arranged to simulate the batch tests, too. The test bottles were assumed to be divided into the anaerobic reactor, corresponding to the liquid phase, and the headspace, corresponding to the gas phase. The unit of the AMPTS II system in which the gases are discharged was simulated as an artificial compartment connected by advective link to the headspace. The increase of volume of the latter compartment would correspond to the volume of biogas produced from the test bottles.

CHAPTER 4.
RESULTS AND DISCUSSION

4.1 Conventional analyses

The results about sample characterisation by conventional analyses are reported in Table 4.1. In the first collection day (April 2019), the mixed sewage sludge was sampled both at the entrance and the exit of the pre-thickening unit. The results about the two samples varied considerably because of the addition of the co-substrate, which has a very different composition from the sludge, to the pre-thickening unit. Despite that, the samples were collected one week later than the last time that the unit was loaded with it. So, it was supposed that no trace of the co-substrate was left in the unit. The composition of the sludge probably changed because an early stage of fermentation took place in the pre-thickener. Hence, the collection in the second day (June 2019) was done again one week later than the last loading of the co-substrate, and the sludge at the entrance of the pre-thickening unit was no longer analysed. It was not possible to extract the soluble fraction of the samples of the co-substrate (named “yogurt”). Therefore, the tests about it were not conducted.

Table 4.1 Characterisation of the samples: a = collected in April 2019; b = collected in June 2019

	Unit	Sludge[a]	Thick sludge[a]	Thickened sludge[b]	Yogurt[a]	Yogurt[b]	Digestate[a]	Digestate[b]
tCOD	g/kg	11,1	30,8	28,4	217	2189	12,7	13,1
TKN	mgN/kg	5389	1919	412	4824	4805	1195	1035
Acetic acid	mg/L	228	1164	1568	2123	3690	82,9	145
Propionic acid	mg/L	27,0	510	376	0,0	30,3	3,35	1,7
Butyric acid	mg/L	25,6	404	372	0,0	252	6,734	44,3
Valeric acid	mg/L	8,4	182	113	0,0	0,0	0,0	0,0
pH	-	7,0	5,5	5,4	4,1	4,1	7,3	7,2
Alkalinity	$mgCaCO_3/L$	760	1139	1002	0	0	3414	3641
TS	g/kg	9,72	24,9	21,0	149	178	12,6	14,3
VS	g/kg	7,14	19,0	16,0	141	151	8,29	9,1
sCOD	mg/L	260	3560	2570	n.a.	n.a.	307	196
sN	mgN/L	30,0	132	119	n.a.	n.a.	586	381
$N\text{-}NH_4^+$	mgN/L	27,0	122	107	n.a.	n.a.	492	380

4.1.1 VFA analyses

The total concentration of VFAs in the samples could be measured by means of different analytical methods. In the laboratory, the concentration of each VFA species (acetate, propionate, butyrate and valerate) was measured by gas chromatography. The unit of measurement of each data was converted into volumetric concentration of COD assuming the stoichiometric coefficients (Table 4.2). Thus, it was possible to sum all the data and calculate the total concentration of VFAs:

$$VFA = \sum_i \alpha_i \cdot \frac{MW_{O2}}{MW_{VFA,i}} \cdot VFA_i$$

Table 4.2 Stoichiometric coefficients used for the COD conversion

VFA_i	α_i
Acetate	2
Propionate	3.5
Butyric	5
Valerate	6.5

Instead, the available data about the total VFAs concentration in the WWTP under study were measured by titration in FOS analysis, which results were expressed in equivalent concentration of acetic acid. Another method to evaluate the total amount of VFAs is by means of the test in kit, which is simpler and faster than the others. The resulting concentrations that could be read in the spectrophotometer are already expressed in equivalent of acetic acid. Therefore, the implicit conversion in the kit test was investigated in order to compare the results among different methods of measurement. Starting from the concentration of each species, the total VFA amount would be calculated as follows:

$$VFA = \sum_i m_{VFA,i} \cdot VFA_i + q_{VFA,i}$$

With m and q equal to the slope and the intercept of the linear fitting curves (Table 4.3 and Figure 4.1).

The accuracy of the estimated conversion coefficients was proved by a set of tests conducted on VFAs mixtures with known composition (relative error ±12%).

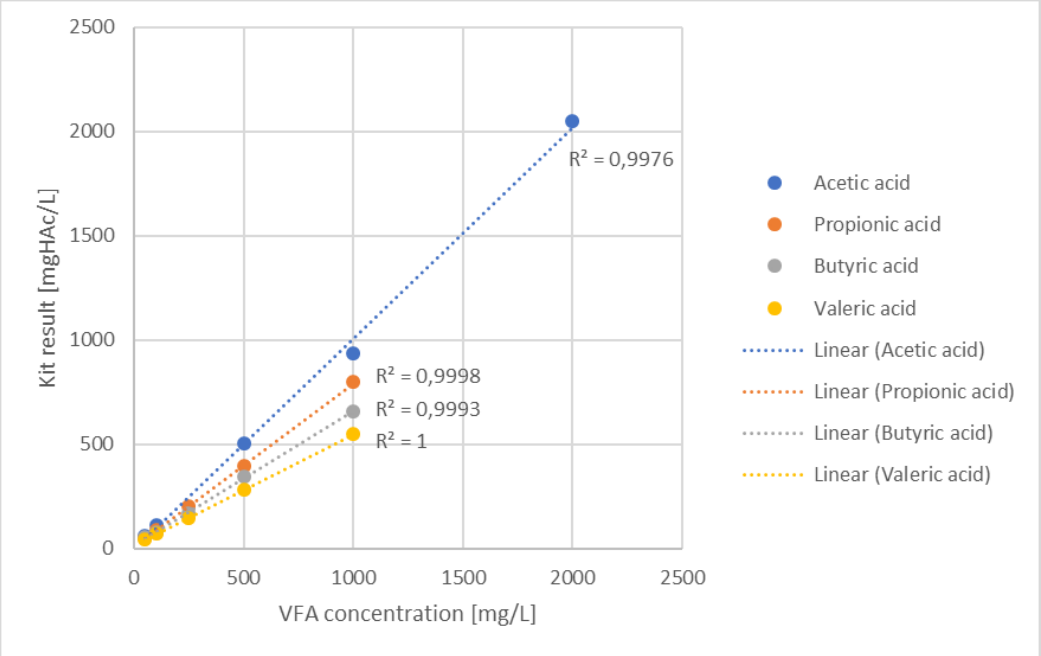

Figure 4.1 Correlation curves for the conversion of the VFAs concentration by gas chromatograph to VFAs concentration by test in kit

Table 4.3 Coefficients of the linear regression fits built comparing the absolute VFA concentrations and the corresponding ones measured by the test in kit

VFA_i	m_i	q_i
Acetate	1,01	-6,83
Propionate	0,79	8,50
Butyric	0,65	16,6
Valerate	0,53	16,6

4.2 Lipids, proteins and carbohydrates analyses

Many authors predicted the composition of the samples based on either VS or COD balance. The most common equations found in literature were [47]:

$$PT(\%COD) = 100 \times \frac{\left[6.25 \frac{g_{PT}}{g_{orgN}} \times (TKN - TAN) \times 1.42 \frac{g_{O2}}{g_{PT}}\right]}{COD}$$

$$LI(\%COD) = 100 \times \frac{\left(LI \times 2.86 \frac{g_{O2}}{g_{LI}}\right)}{COD}$$

$$CH(\%COD) = 100 - PT(\%COD) - LI(\%COD)$$

However, many approximations were considered in these equations. First, the conversion factor of organic nitrogen (evaluated as the difference between the TKN and the Total Ammonia Nitrogen, mostly NH_4^+) to protein is an estimation based on the average N content in proteins. Similarly, the conversion factors to COD could vary as the molecules included in proteins and lipids are numerous. Finally, not all the COD content of the sample should be attributed just to CH, PT and LI, because there might be other molecules such as alcohols and acids. Therefore, alternative methods relying on the direct estimation of each single component was tested. As for the conversion between mass and COD of each component for carbohydrates, the stoichiometric coefficient used in the the Dubois method was used i.e. the one for glucose (1.067 $g_{COD}/g_{GLUCOSE}$). In the case of proteins, the COD coefficient was directly derived from the measurements of sCOD on the BSA standard (1.485 g_{COD}/g_{BSA}). Instead, the direct assessment of this conversion for lipid was not feasible and the COD coefficient found in literature was used (2.86 $g_{COD}/g_{LI,VS}$).

4.3 Hydrolysis techniques

The sensitivity of each pre-treatment method was checked using cellulose as the reference carbohydrate (Table 4.4). Only 35.6% of the cellulose content was hydrolysed when the samples were simply diluted with deionised water and the Dubois method was directly applied. The dilution of the samples with HCl and the following digestion let 66.3% of the theoretical carbohydrate content hydrolyse. 78% of the cellulose was hydrolysed when the samples were diluted with deionised water and then sonicated. Instead, the same pre-treatment as in the procedure to measure TKN and the sonication process in the solution of sulphuric acid could not be completed because they interfered with the colorimetric analysis. According to these results, the dilution with deionised water followed by sonication was selected as the most efficient pre-treatment to hydrolyse the sample and so to detect its total carbohydrate content. Although the measured content never reached the expected one, the percentage of hydrolysed cellulose obtained by sonication is similar to the amount that is usually anaerobically degraded in BMP tests conducted on cellulose found in literature.

Table 4.4 Results of the tests on the sensitivity of the hydrolysis pre-treatment; the method number is referred to the list that can be found in Materials and Methods

Method	Expected carbohydrate content [mg/L]	Measured carbohydrate content [mg/L]
Simple dilution (1)	200	71,3
HCl digestion (3)	100	66,3
Water sonication (4)	100	78,0

However, the nature of the sample was expected to affect the efficacy of the pre-treatment. So, every method (apart from the hydrolysis prior to TKN measurement) was tested on the sludge samples too. A sample of pre-thickened sludge from the WWTP in Sesto San Giovanni was studied. As expected, sonication was the most effective pre-treatment (Figure 4.2). The difference between the results obtained by diluting the sample with deionised water and with sulphuric acid was less than 3%. The treatment of sulphuric acid was considered to be more dangerous to be implemented by the operator than the other methods; moreover, more acid is added to implement the Dubois method. Therefore, dilution of the sample with deionised water followed by sonication was considered as the best hydrolysis pre-treatment.
Additional errors might be caused by using cellulose acetate filters to filter the sample and separate the soluble fractions. During the extraction, the filters could release some cellulose in the sample, interfering with the measurement. Therefore, a blank filtered on cellulose was added in the case the sample that was tested was also filtered.
Furthermore, the possibility that the content of the sample, that in the case of sludge is very complex, could directly interfere with the evaluation of the carbohydrate content by adding the reagents of the Dubois method was investigated. In order to do that, the samples of pre-thickened sludge that were already sonicated were additionally spiked with a fixed amount of glucose (and computed in order to fall within the calibration range of the Dubois method). The results showed a slightly different concentration of carbohydrates from the expected one (-13%). Therefore, it was deduced that the components released by the sludge could interact with the Dubois method, causing interferences. However, this interference is low enough to be considered as acceptable.

Finally, both pre-thickened sludge, co-substrate (“yogurt”) and digestate sludge samples that have been collected in June 2019 were pre-treated by sonication and their carbohydrate content was measured by Dubois method. The tests were conducted in triplicate (both on the total and on the soluble fractions). Results are summarised in Table 4.5.

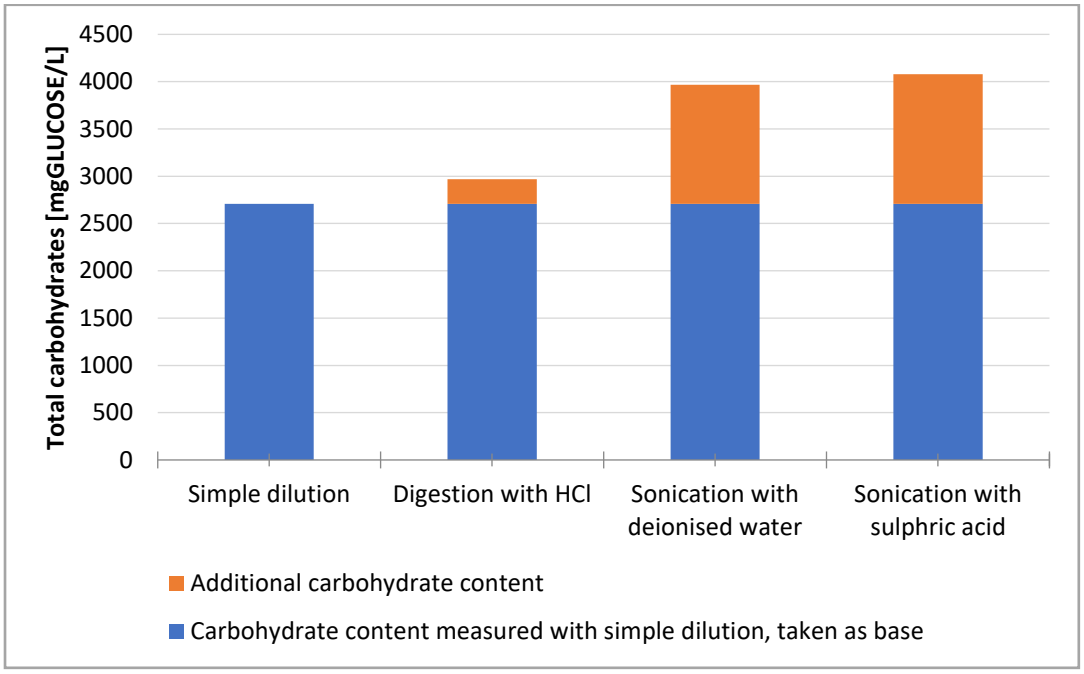

Figure 4.2 Measurements of the total carbohydrate concentration of the same sample that have been hydrolysed by different methods

Table 4.5 Summary of the analyses on carbohydrates of the collected samples in June 2019

Sample	Fraction	Carbohydrate content	Unit	Coefficient of variation
Pre-thickened sludge	soluble	17,1	mg/L	4%
	total	2,63	g/L	8%
Yogurt	total	142	g/L	4%
Digestate sludge	soluble	9,36	mg/L	3%
	total	1,25	g/L	5%

The total fraction of carbohydrate of the pre-thickened sludge showed the highest variability. Nevertheless, it was smaller than 8%, so the repeatability of the procedure was satisfactory.
The protein content was evaluated by the BCA method on the same samples that have been pre-treated by sonication (Table 4.6). In this case, the results about the soluble fraction of the digestate sludge showed a great variability (27.5 %). This might be related to the high slope coefficient that is derived from the calibration curve. However, the average variability of the results for the other samples was lower than 6%.
The pre-treatment was not applied to the samples for the measurement of the lipids content, since the relative method did not require it (Table 4.7). Unfortunately, the soluble fractions of lipids were not available due to scarcity of samples. Indeed, at least 200 mL of 0.45 µm filtered

sample were needed for lipid extraction from the liquid phase. This sample preparation phase may become very time consuming depending on the TS content of the sludge.
Contents of sludges were comparable to literature values ([36], [44], [50]).
As one more check on the experimental results, data obtained for the yogurt were compared with those reported as the average of the nutritional values on the labels of a set of yogurt packages. This comparison is shown in Table 4.8. These data suggested that the methods that were adopted to measure the carbohydrates and proteins content well-approximate the real values. Instead, the method for extracting the lipids underestimates the real content.

Table 4.6 Summary of the analyses on proteins of the collected samples in June 2019

Sample	Fraction	Protein content	Unit	Coefficient of variation
Pre-thickened sludge	soluble	114	mg/L	5%
	total	8,37	g/L	4%
Yogurt	total	35,6	g/L	6%
Digestate sludge	soluble	19,6	mg/L	27%
	total	7,81	g/L	1%

Table 4.7 Summary of the analyses on lipids of the collected samples in April 2019

Sample	Fraction	Lipid content	Unit
Pre-thickened sludge	total	2,57	g/L
Yogurt	total	6,10	g/L
Digestate sludge	total	0,57	g/L

Table 4.8 Average nutritional values of a set of yogurt samples

	Content [g/100 g]	Content [g/L]
Carbohydrates	10,8	135
Proteins	3,16	39,5
Fats	2,96	37,0

4.4 Anaerobic biodegradability and activity tests

4.4.1 Specific Methanogenic Activity tests

The SMA value was calculated as the maximum methane production (specific to the VS content of the inoculum) in the unit of time. Observing the plot of the data about methane production recorded by the AMPTS II software (Figure 4.3), the SMA could be computed from the maximum slope of the curve over a subset of data where it was approximately constant. In this case, an interval of 5 hours after 20 hours of run was considered. A buffering period of at least half a day was allowed at the beginning of the test. The SMA values are reported in Table 4.9. The results were comparable to literature values ([51], [52]). Since the acetoclastic archea prevails over hydrogen-utilising organisms in the methanogenesis process, the SMA value corresponds to the maximum organic loading rate that they can sustain.

Table 4.9 Results of the SMA test

Data	Unit	Average
Hourly CH4 production	NmLCH4/h	10,3
SMA	NmLCH4/(gVS*d)	60,4
	gCOD/(gVS*d)	0,173
SMA literature	gCOD/(gVS*d)	0,135

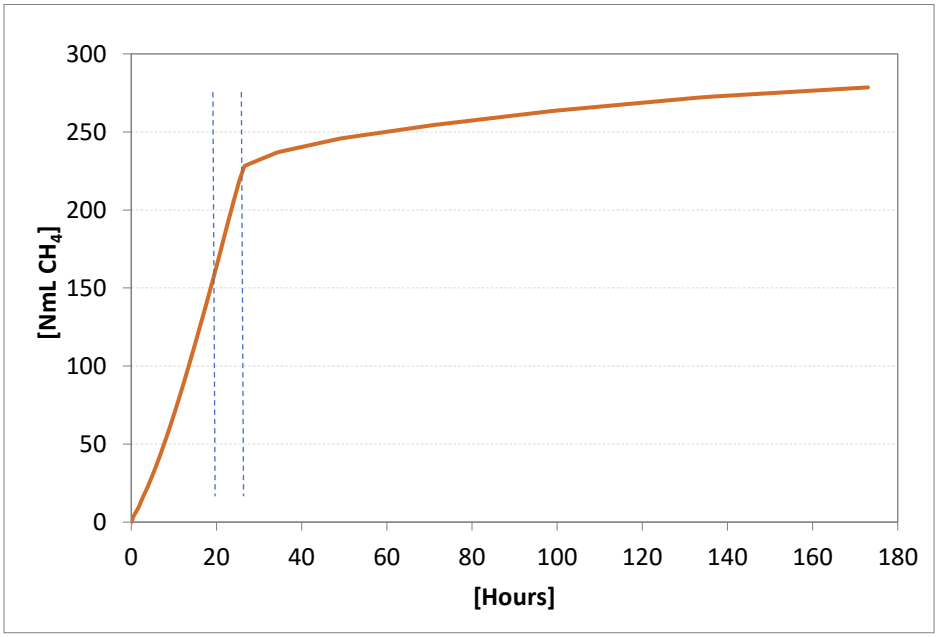

Figure 4.3 Cumulative gross methane production during the SMA test; the dashed lines identify the interval of time in which the SMA value was evaluated

4.4.2 Biochemical Methane Potential tests

The biodegradability capacity of the digestate coming from the WWTP under study was investigated. The activity of acidogenic and acetogenic bacteria, specifically the sugar degraders, was assessed by means of a BMP test with glucose as substrate. Glucose is already solubilised, so its digestion does not involve the disintegration and hydrolysis steps. Blank tests were conducted in order to measure the endogenous methane production of the inoculum. Hence, the specific methane production from the substrate was calculated as the net amount of the total production and the endogenous one. The test was not satisfactory compared to what is reported in the standard UNI/TS 11703 (2018) since the variability exceeded the threshold assumed for soluble substrates (5%). However, the batch test was relevant to discuss the evolution of the methane production over the test period (39 days). The cumulative methane production curve was built plotting the data recorded daily by the AMPTS II software (Figure 4.4). No lag time was needed to the biomass to start the methane production, as glucose is a soluble and easily fermentable substrate. The peak of production (38.9 $NmL_{CH_4}/g_{VS,inoculum}/d$) was reached in two days. Then, the rate dropped down. Despite that, the production of methane never stopped over the test period. The average methane yield and biodegradability values are reported in Table 4.10.

On the opposite, cellulose is not readily degradable. Hence, a BMP test was conducted with cellulose as substrate in order to assess the disintegration and hydrolysis capacity of the biomass in the digestate sludge. The production of methane associated to the substrate started with delay, as the total amount of methane that has been produced in the beginning of the test was like the endogenous production. The peak of production rate (41.2 $NmL_{CH_4}/g_{VS,inoculum}/d$) was reached in day 3 (Figure 4.5). Then, the production rate dropped, and it reached almost zero after two weeks that the test started because all the COD content of the substrate was degraded. The methane yield and biodegradability values are reported in Table 4.11. The coefficient of variability of the test was considered satisfying for a not-soluble substrate like cellulose.

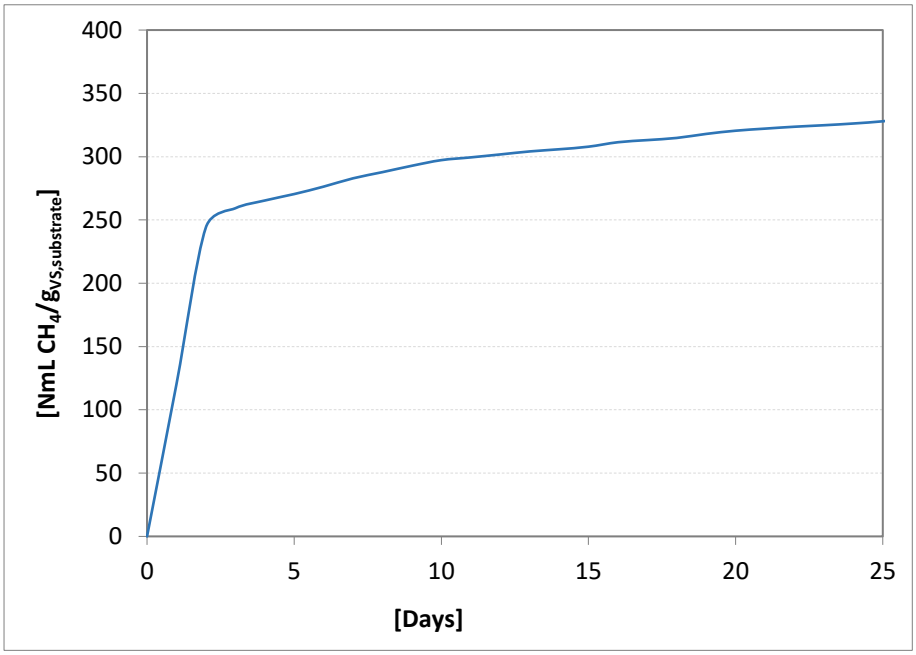

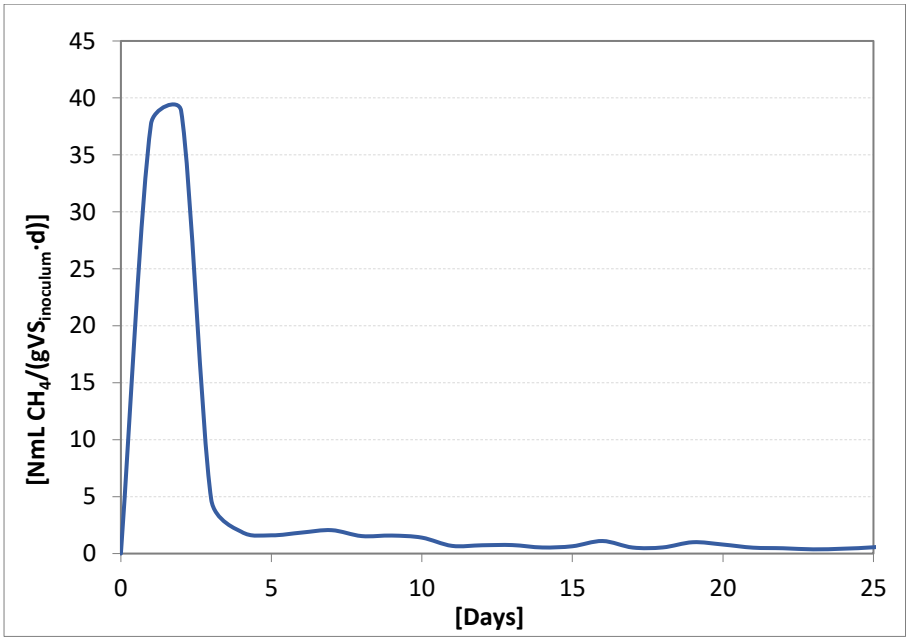

Figure 4.4 Plot chart of the cumulative net methane production in the BMP test with glucose as substrate (above); specific methane production rate (below)

Table 4.10 Methane yields resulting from the BMP test with glucose as substrate

BMP unit	Mean	Standard deviation	Variability
NmLCH4/gCOD,substrate	345	45,2	13,1%
NmLCH4/gTQ,substrate	368	48,2	13,1%

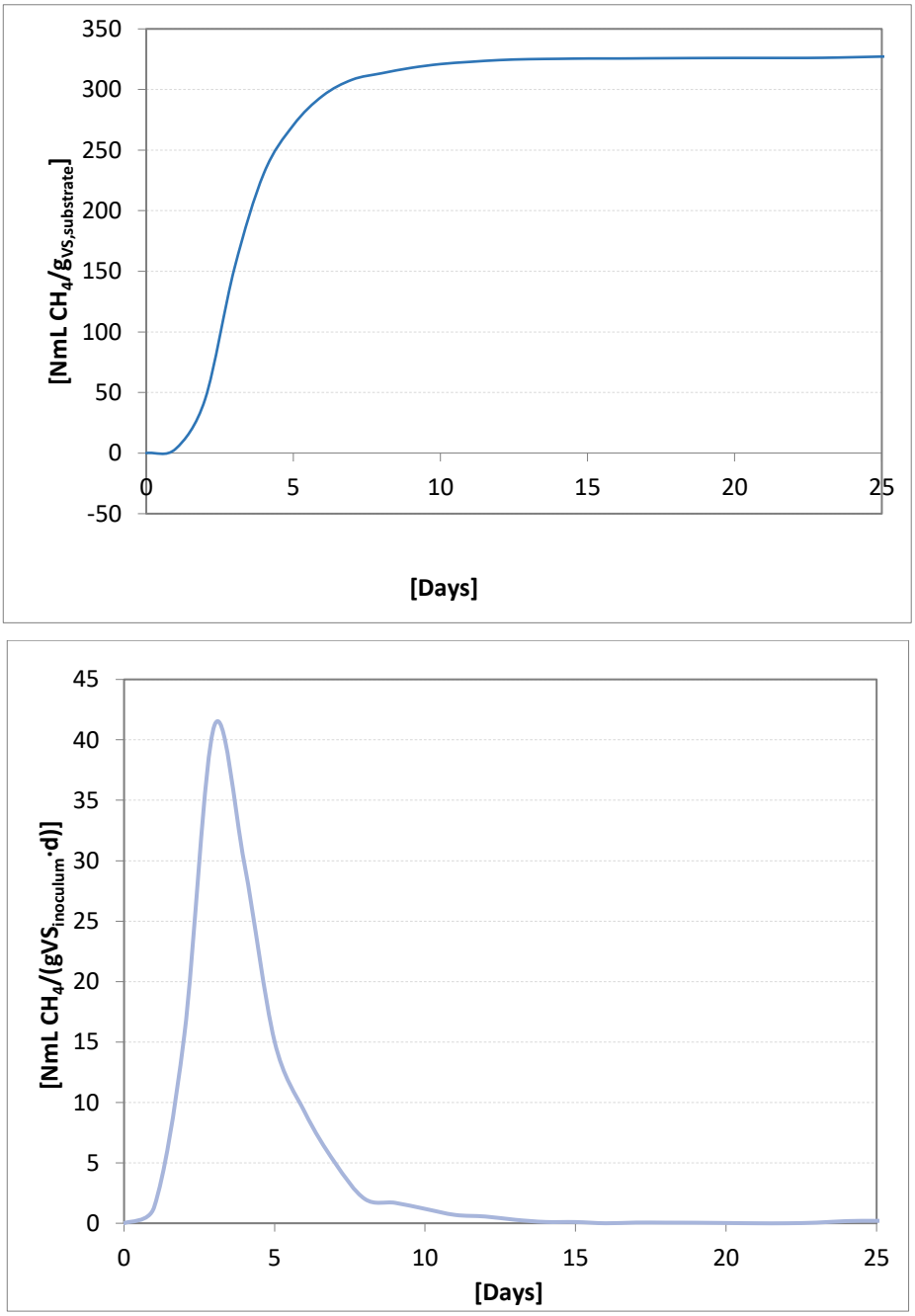

Figure 4.5 Plot chart of the cumulative net methane production in the BMP test with cellulose as substrate (above); specific methane production rate (below)

Table 4.11 Methane yields resulting from the BMP test with cellulose as substrate

Unit	Mean	Standard deviation	Coefficient of variation
mLCH4/gVS,substrate	328,2	23,5	7,17%
mLCH4/gTQ,substrate	309,99	22,23	7,17%

A set of BMP tests was conducted about the co-substrate of the real WWTP. In the laboratory experiments, a mixture of dairy products (especially different kinds of yogurt) coming from the plant was used. The dilution ratio of the yogurt in the test bottles was assumed such that inhibition would not occur. The test was set up adopting a ISR of 4.1 $g_{VS,inoculum}/g_{VS,substrate}$. This low loading condition resulted in a short BMP test (Figure 4.6).
In the second experiment, the amount of dilution water in the bottles was increased and the ISR was 3.5 $g_{VS,inoculum}/g_{VS,substrate}$, similar to the previous test.

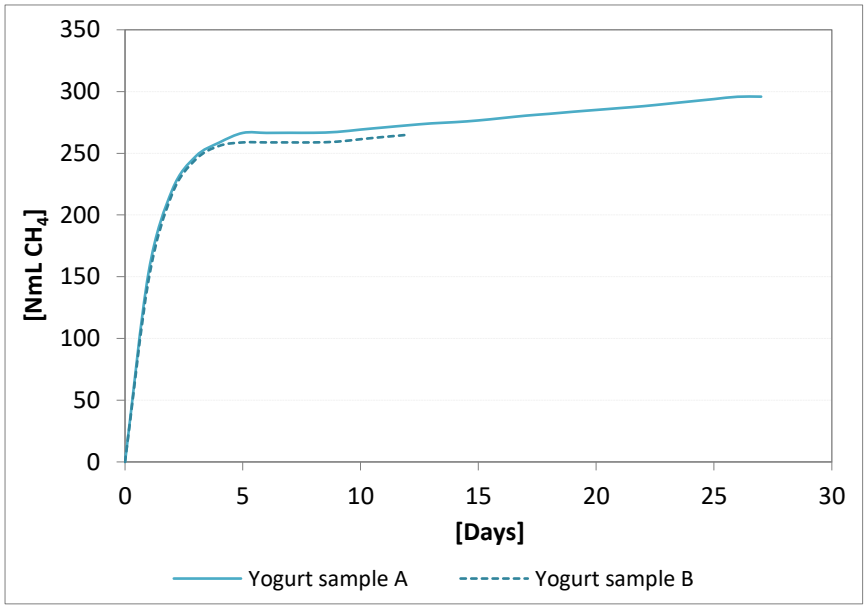

Figure 4.6 Plot chart of the cumulative net methane production in the BMP test with yogurt as substrate; it can be noticed that the test of one bottle stopped earlier

Finally, a BMP test was conducted on pre-thickened sludge as substrate. Bicarbonate (1 g) was added to each experimental bottle to increase the pH of the mixture to 7.2. The test lasted for 26 days. In the beginning of the experiment, the rate of production in the samples with sludge resulted slightly slower than with yogurt. Moreover, the production dropped to zero faster in the case of yogurt (Figure 4.7). These results complied with the assumption that yogurt could be degraded faster than sludge. Moreover, yogurt could produce more methane than sludge (Figure 4.8) because of its higher organic content. Indeed, the C/N ratio of the liquid phase could be adjusted to optimal values thanks to addition of the co-substrate. The results of the BMP tests are summarised in Table 4.12.

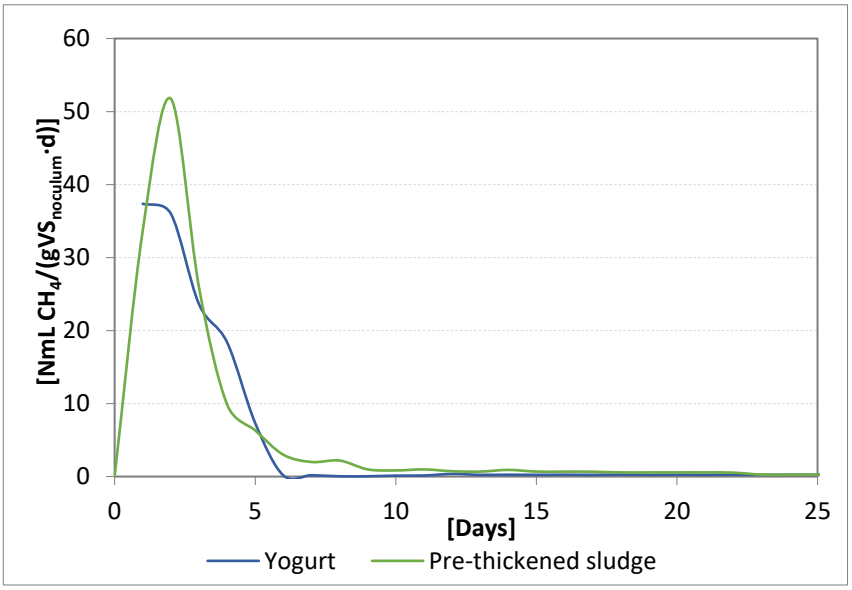

Figure 4.7 Specific methane production rate

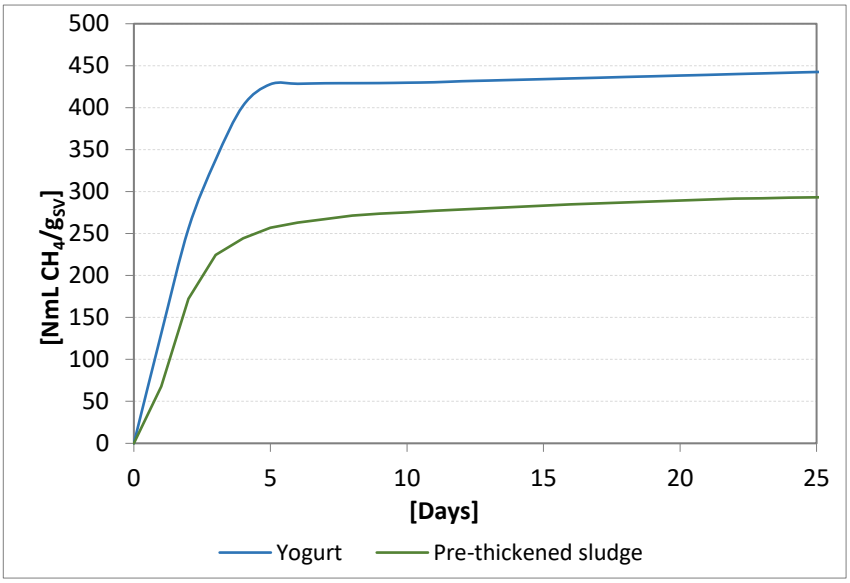

Figure 4.8 Plot chart of the cumulative net methane production in the BMP test with cellulose as substrate

Table 4.12 Methane yields resulting from the BMP tests with yogurt and pre-thickened sludge

Sample	Unit	Mean	Standard deviation	Coefficient of variation
Yogurt	mLCH4/gVS,substrate	442	10,8	2,45%
	mLCH4/gTQ,substrate	66,6	1,6	2,45%
Pre-thickened sludge	mLCH4/gVS,substrate	293	1,4	0,47%
	mLCH4/gTQ,substrate	4,7	0,0	0,47%

However, the addition of yogurt should be calibrated in order to avoid excessive accumulation of VFAs in the liquid phase. A slight acidification in the bottles with yogurt was observed in the BMP test since the final pH value dropped to 7.0. Additional tests would be required to investigate the right ratio between the two kinds of substrate, pre-thickened sludge and yogurt, in order to adjust the loading in the real plant and improve the anaerobic process. However, similar evaluations could also be discussed base on simulations with the ADM model, as discussed in the following paragraph.

4.5 Implementation of the ADM1

The first issue when using the ADM model is to assign the correct value to all relevant state variable in the influent. These values were defined by using the results of the chemical characterization on the substrates that were conducted in the laboratory A. Rozzi. In accordance with the model requirements, all the variables were expressed as kg COD/m3, apart from carbon, nitrogen and any ionic compound that were expressed as molar concentration (kmol/m3 or M). Many assumptions were done because some data could not be directly measured. Indeed, they were either derived from mass balances or assumed from the literature.

The concentration of hydrogen ions (*S_h_ion*) was derived by the measured pH value.

$$S_{h_{ion}} = 10^{-pH}$$

From the results about alkalinity, the concentration of bicarbonate (*S_hco3_ion*) was calculated, and it was used to derive the concentration of inorganic carbon (*S_IC*) and carbon dioxide (*S_co2*) by the equation of acid-base equilibrium.

$$S_{hco3}\left[\frac{kg\ COD}{m^3}\right] = \frac{Alk\ \left[\frac{mg\ CaCO_3\ eq}{L}\right]}{50\ [g\ CaCO_3\ eq]\cdot 1000}$$

$$S_{IC} = S_{hco3}\cdot\frac{K_{a,co2} + S_{h_{ion}}}{K_{a,co2}}$$

$$S_{co2} = S_{IC} - S_{hco3_{ion}}$$

The concentration of total inorganic nitrogen (*S_IN*) was derived from the ammoniacal nitrogen content of the samples.

$$S_{nh4} = \frac{NH_4^+ \left[mg\frac{N}{L}\right]}{14\left[\frac{kg}{kmol}\right] \cdot 1000}$$

The concentrations of ammonium (*S_nh4_ion*), free ammonia (*S_nh3*) and the dissociate fractions of each VFAs (*S_ac_ion*, *S_pro_io*, *S_bu_ion*, *S_va_ion*) were calculated according to the acid-base equilibrium equations reported in ADM1 (Appendix A).

The value of the net charge of all other ions (*S_delta_ions*) was calculated by satisfying the charge equilibrium.

$$S_{delta_{ions}} = S_{hco3_{ion}} + \frac{S_{ac_{ion}}}{64} + \frac{S_{pro_{ion}}}{112} + \frac{S_{bu_{ion}}}{160} + \frac{S_{va_{ion}}}{208} + S_{oh_{ion}} - S_{nh4_{ion}} - S_{h_{ion}}$$

The concentration of soluble inert (*S_I*) was derived from the balance of the soluble COD. The concentration of fatty acids was assumed to be equal 5% of the particulate lipids since it was not possible to measure the relative soluble fraction.

$$S_I = sCOD - S_{su} - S_{aa} - S_{fa} - S_{ac} - S_{prp} - S_{bu} - S_{va}$$

The sludge in the influent to the anaerobic reactors was assumed to be composed of a mixture of primary sludge (60% of the total COD content at input) and secondary sludge (40%). The two types were defined differently. The primary sludge was assumed to be already disintegrated, so no composite (*X_c*) was in it. Instead, the secondary sludge was assumed to be composed only of composite particulate organics. Therefore, the content of particulate inerts (*X_I*) and composite were derived from the particulate COD balance on primary and secondary sludge, respectively.

$$pCOD = COD - sCOD$$

$$X_c = pCOD - X_{ch} - X_{pr} - X_{li}$$

$$X_I = pCOD - X_{ch} - X_{pr} - X_{li}$$

The disintegration fractions of the composite were derived from the breakdown of the particulate COD, too (Table 4.13). It was assumed that not all the composite could be degraded, but 15% (for assumption) of it would result as inert.

Table 4.13 Disintegration coefficients: a = Batstone et al., "Anaerobic Digestion Model No.1 (ADM1) IWA Scientific and Technical Report No. 13" (2002); b = Rosén and Jeppsson, "Aspects on ADM1 implementation within the BSM2 framework" (2006)

f_Xc (kg COD/kg COD)	ADM1[a] constants	Rosén[b] constants	Experimental values
Carbohydrates	0,20	0,20	0,09
Proteins	0,20	0,20	0,43
Lipids	0,25	0,30	0,02
Soluble inerts	0,10	0,10	0,00
Particulate inerts	0,25	0,20	0,46

The experimental values conflicted with the default parameters. The cause for that could derive from errors in the methods adopted to characterise the samples (the proteins content was apparently overestimated, the lipids content underestimated) or errors in the conversion of the results to COD. In future studies, the proteins content could be derived from the TKN value, adjusting the coefficient that was found in literature. Additionally, a different solvent from hexane could be adopted in the procedure to extract lipids and measure their content.
The co-substrate ("yogurt") variables were defined alike. As it is readily degradable, it was assumed to not contain composite. Therefore, the disintegration fractions were not calculated for yogurt.
Then, all the stoichiometric, biochemical and physiochemical parameters were assumed from the report of Rosén and Jeppsson as initial values to perform the full-scale simulation (Appendix C). Additionally, the composition of the sludge already present in the anaerobic digester at the initial time was assumed as the default values in ADM1, because the simulation was performed over a period greater than 3 times of the HRT (30 days in the case under study).
The data about the operation of the WWTP in Sesto San Giovanni in the years 2016 and 2018 were released by the operator CAP. However, the plant was turned off during most of days in 2018, so only the data about the operation in 2016 were utilized in the simulation. The compartments in AQUASIM 2.0 were sized according to the real plant (Table 4.14). The historical data about loadings and biogas production were used in input to the model.

Table 4.14 Sizing of the full-scale digester in the WWTP under study

Compartment	Volume (m^3)
Anaerobic reactor	2000
Headspace	400
Gasometer	800

The outlet reactors (one for each anaerobic digester) were created to simulate the compartments in which the digestate sludges from both reactor A and B are discharged. Neither the initial conditions nor the input loadings of the outlet reactors were described since they were connected to the corresponding digester by advective links.

An artificial flowrate was added as input of each headspace to simulate the gasflow exiting because of overpressure in the compartment (reactor with constant volume, so the exiting flowrate must be equal to the entering one, see Appendix D).

The operation of the full-scale plant was simulated for one year (365 days) assuming to be loaded as in January 2016 on average. In this way, the system in AQUASIM 2.0 did not show transient conditions when the simulation continued for an additional year (365 days, referred to 2016) with the same loading conditions as in the real plant. The simulation was extended by 60 days with constant loading in order to obtain steady-state output values. The simulation of digester A was not evaluated since it was off most of the year (2016) and its operation showed great variability.

As first attempt, the simulation of the full-scale digester was run assuming the hydrolysis constants as in the report of Rosén and Jeppsson (k_{hyd} = 10 d^{-1}). From the results, there was clear evidence that the parameter was overestimated because the simulated biogas production was far from the real data points. Therefore, k_{hyd} was adjusted to 1 d^{-1} in agreement with the parameters for AD of sludges in continuous conditions that can be found in the report of the IWA Task Group. The Theil's Inequality Coefficient (TIC) was used to evaluate the fitting of the simulated data points and the measured data points.

$$TIC = \frac{\sqrt{\sum_i (y_i - y_{m,i})^2}}{\sqrt{\sum_i {y_i}^2} + \sqrt{\sum_i {y_{m,i}}^2}}$$

With y_i representing the simulated data points and $y_{m,i}$ representing the measured data points. Zhou (1993) reported that a value of the TIC lower than 0.3 indicates a good agreement with measured data [53].

The simulated biogas production and pH showed a good data fitting (see figure, TIC equal to 0.156 and 0.014, respectively). On the contrary, simulated alkalinity and volatile acids were not in accordance with the measured data (TIC equal to 0.391 and 0.323). Errors in the evaluation of alkalinity put in input in the model could derive from the errors in the evaluation of the proteins content of the sludge samples.

Moreover, inhibition could be evaluated thanks to the variable that are calculated during the simulation. The inhibition of acetoclastic methanogens by free ammonia affected the most the system (Figure 4.10).

The concentration of methane in the gasometer resulted very poor (50% on average). This could still derive from errors in the characterisation of the input, most probably due to the very low content of lipids that was measure.

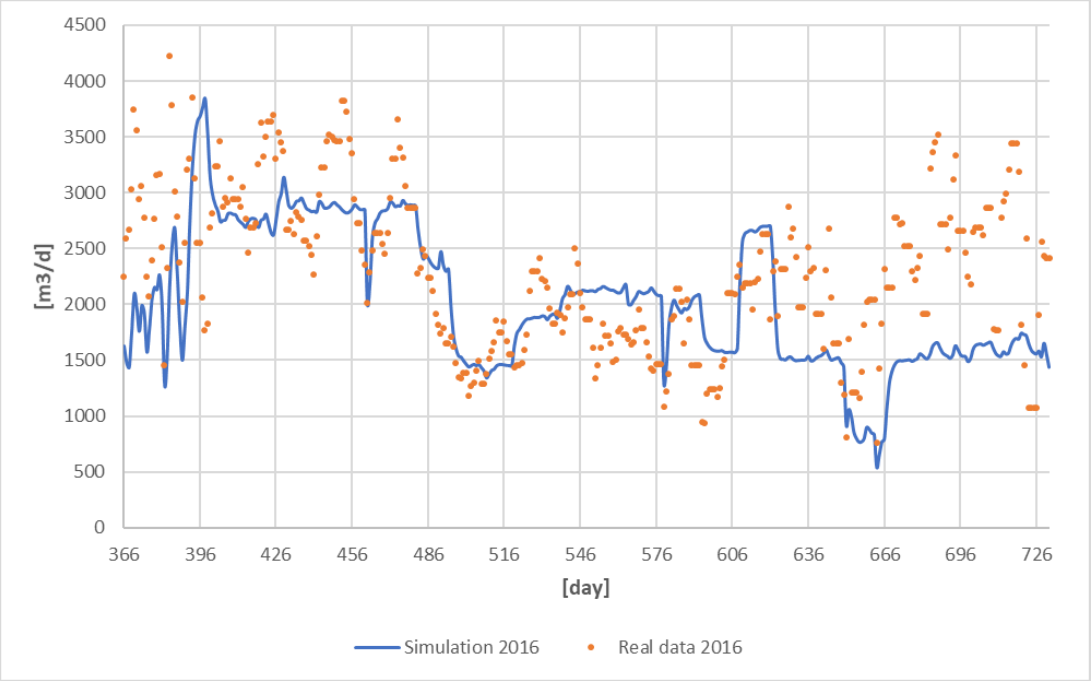

Figure 4.9 Biogas production in the year 2016 according to the simulation in AQUASIM

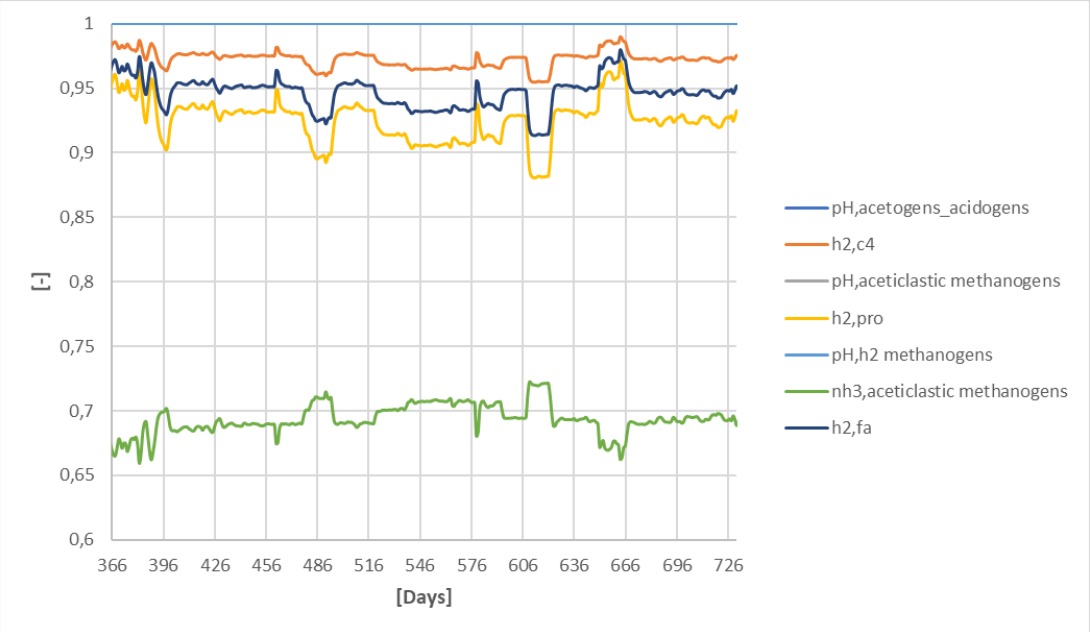

Figure 4.10 Values of inhibition factors in the simulation of the liquid phase of reactor B

Finally, an additional indicator was evaluated to quantify the efficiency of the biological system to transfer COD content from the substrate to methane.

$$Efficiency = \frac{Sch4 \cdot Gasflow}{TotalCOD \cdot Qloading}$$

The efficiency of the simulated system, considering only the interval of time corresponding to the operation of the full-scale digester in 2016, was equal 0.51.

Therefore, some kinetic parameters were adjusted in accordance to the experimental results that were obtained in the laboratory. The batch tests were simulated in AQUASIM based on the ADM1. The AD process was investigated starting from the bottom steps in it. Thus, the variables of the SMA test were uploaded to the system. The addition of the substrate was simulated as a load that have been charged to the anaerobic reactor before that the simulation started. The characterisation of the inoculum in the test bottles was assumed to be equal to the composition of the digestate in the full-scale reactor when steady state was reached. All the dynamic processes in the anaerobic digester were inactivated apart from the uptake of acetate. The volume of the gases that were transferred from the headspace to the outlet reactor was adjusted to normal conditions (Appendix D). The simulation was run with steps shorter than 1 (day) in order to evaluate the simulated data with more precision. The amount of methane that was produced and accumulated in the outlet reactor was calculated assuming that the same equations of the system in continuous were valid.

No correlation could be found between the measured data and the simulated ones. Most probably, additional parameters in the simulation platform needed to be adjusted for batch tests. In fact, ADM1 is a very stiff model because it contains a large range of time constants. So, some system states react quickly whereas some react slower. This was reflected into the incorrect simulation of the batch tests (both SMA and BMP) due to the short time of simulation.

CHAPTER 5.
CONCLUSIONS AND PERSPECTIVES

Many studies have evidenced the benefits that can derive from the addition of a co-substrate at the inlet of an anaerobic digester. The improvement that can be achieved is remarkable when codigestion is applied to poor systems. This is the case of the anaerobic digesters that already exist in the treatment line for sludges in the Wastewater Treatment Plants. Modelling is a beneficial tool to understand the biological processes that happen during anaerobic treatment, and so to improve their performance.

Therefore, in this study it was tried to model the past operation of the full-scale anaerobic digester in the WWTP owned by CAP in Sesto San Giovanni in order to simulate its functioning when codigestion is applied. Among the available literature, it was chosen the ADM1 by the IWA Task Group because of its robustness.

Nonetheless, the application of the already existing model revealed many obstacles. The theoretical description of the biological and physico-chemical processes reported in the model was correct. Though, numerous variables and parameters were required at the input of the model. The data that could be collected in the laboratory and in the real plant were not enough to completely fulfil the variables of the model. Therefore, many assumptions were done, and many parameters were assumed from literature. It was not possible to evaluate the accuracy of each of them.

In particular, the AD model lacked a unified method to measure the carbohydrates content. Different methods that have been found in the literature were tested. The application of sonication to the samples of sewage sludge, digestate and yogurt (dilution 1:1 with deionized water) resulted as the method that better hydrolyse the sample, and so the most suitable for measuring the total carbohydrate content in solid matter. The same pre-treatment was adopted in the evaluation of total proteins content, and the results were in accordance with the literature. Instead, the lipids contents were underestimated with respect to the average values. Thus, the applied method to measure lipids should be correct or a new one should be adopted. Additionally, the COD conversion factors of the standards that were used in the calibration of the methods to measure carbohydrates and proteins were proven, while it was not possible to verify the ones referred to lipids.

Another assumption that was made in this study was about its conventional characterisation. Indeed, the contents of sludge have a great variability due to its nature. The composition of biological systems is very sensible to the ambient conditions. Therefore, a greater amount of analyses should be conducted in order to create a dataset that is large enough to identify the

closest composition of the samples to the real one. Because of that, the model should include the simulation of the seasonal variation of the composition of the sludge that is treated in the WWTP. As example, the sludge would be more diluted in the raining seasons, or the composition of the anaerobic inoculum would be affected by the external temperature if the digester is not insulated properly. Even though, unpredictable changes in the composition would affect the simulation results.

The AQUASIM 2.0 platform was a powerful tool. Thanks to it, all the processes that were described in the ADM1 could be described and simulated for a large interval of time. The results of the simulation of the biogas production in the full-scale digester were in accordance with the historical measured data in the real plant. Nevertheless, some simulated variables did not comply with the measured data.

The implementation of the system in AQUASIM 2.0 should be furtherly studied in the case batch systems would be simulated. From that, it would be possible to estimate the kinetic parameters and adjust them in the model used for simulating a full-scale system.

It was concluded that the composition of the system at input mainly affect the simulation. In particular, it was assumed that the simulated value of alkalinity was higher than the measure value because the protein content was overestimated. Thus, the hydrolysis pre-treatment should not be applied to the samples of the BCA test.

Moreover, the simulated ammonium concentration resulted higher than expected. A high content of nitrogen should increase the production on methane. Instead, it was observed a poor content of methane in the biogas during the simulations, both in continuous and batch mode. The cause of that was addressed to the underestimation of lipids.

Nonetheless, taking some precautions, the application of ADM1 to the full-scale digester could be useful to predict the biogas production when a co-substrate is added to the reactor. In the real plant, some discarded dairy products are already recovered in the AD process. The anaerobic biodegradability of the co-substrate was evaluated in this thesis. The batch test revealed that “yogurt” is a valuable substrate as it has a higher organic content and it is degraded faster than the sludge. However, the amount that is added to the reactor should not overcome a certain threshold, otherwise the synergistic effects of codigestion would transform antagonistic effects. Accumulation of VFAs and subsequent inhibition of the AD process are the main ones. Therefore, the models of batch tests could be developed to simulate the BMP tests of both “yogurt” and pre-thickened sludge. The simulation would be useful to adjust the ratio between different substrates they are co-digested in order to achieve the best performance of the system. Thanks to that, the simulation of the system in continuous mode would predict the potential biogas production in full-scale application.

In the end, additional improvements could be done to the system that was implemented. The AQUASIM 2.0 platform could be used to simulate the treatment of the sludge in the other units that are present in the WWTP. In particular, the simulation of the AD process would be

improved if the biological system is described also in the pre-thickening unit. Indeed, from the analyses of the samples that were collected in the plant, it was supposed that an early stage of fermentation occurs in it.

Ringraziamenti

Questa tesi conclude un percorso di studi che è stato essenziale per la mia formazione e crescita. Quindi, grazie a mamma e nonna che hanno contribuito perché io ricevessi un'istruzione così elevata, vicino e lontano da casa.
Devo ringraziare la Professoressa Elena Ficara, Arianna Catenacci e Nadia per avermi accolto nel loro laboratorio, aver avuto pazienza a rispondere a tutti i miei dubbi, e avermi sempre stimolato nonostante gli ostacoli.
Grazie alle mie migliori amiche Kia, Marti e Minni. Le distanze non ci hanno mai separate, e siete sempre state in grado di essermi di conforto.
Grazie alle Chicas per aver condiviso con me ogni momento di questa Laurea Magistrale, e avermi fatto diventare un po' latina, nonostante io non parli ancora lo spagnolo.
Non vanno dimenticati i mitici compagni della Classe E, del KAIST, tutte le coinquiline e le persone con cui ho passato anche solo una festa assieme. Se non vi avessi incontrato, non sarei la stessa persona.

Bibliography

[1] Metcalf & Eddy Inc., *Wastewater Engineering - Treatment and Resource Recovery*, Fifth Edition. McGraw-Hill Education, 2013.

[2] S. Longo *et al.*, 'Monitoring and diagnosis of energy consumption in wastewater treatment plants. A state of the art and proposals for improvement', *Applied Energy*, vol. 179, pp. 1251–1268, 2016.

[3] Y. Gu *et al.*, 'Energy self-sufficent wastewater treatment plants: feasibilities and challenges', *Energy Procedia*, vol. 105, pp. 3741–3751, 2017.

[4] J. Xu, Y. Li, H. Wang, J. Wu, and F. Li, 'Exploring the feasibility of energy self-sufficient wastewater treatment plants. a case strudy in easter China', *Energy Procedia*, vol. 142, pp. 3055–3061, 2017.

[5] R. Kollman *et al.*, 'Renewable energy from wastewater - Practical aspects of integrating a wastewater treatment plant into local energy supply concepts', *Journal of Cleaner Production*, vol. 155, pp. 119–129, 2017.

[6] J. Henriques and J. Catarino, 'Sustainable value - An energy efficiency indicator in wastewater treatment plants', *Journal of Cleaner Production*, vol. 142, pp. 323–330, 2017.

[7] Y. Shen, J. J. Linville, M. Urgun-Demirtas, M. M. Mintz, and S. W. Snyder, 'An overviw of biogas production and utilization at full-scale wastewater treatment plants in the United States: Challenges and oppportunities towards energy-neutral WWTPs', *Renewable and Sustainable Energy Reviews*, vol. 50, pp. 346–362, 2015.

[8] H. Guven, R. K. Dereli, H. Ozgun, M. E. Hersahin, and I. Ozturk, 'Towards sustainable and energy efficient municipal wastewater treatment by up-concentration of organics', *Progress in Energy and Combustion Science*, vol. 70, pp. 145–168, 2019.

[9] W.-W. Li and H.-Q. Yu, 'Advances in energy-producing anaerobic biotechnologies for municipal wastewater treatment', *Engineering*, vol. 2, pp. 438–446, 2016.

[10] Y.-J. Liu, J. Gu, and Y. Liu, 'Energy self-sufficient biological municipal wastewater reclamation: Present status, challenges and solutions forward', *Bioresource Technology*, vol. 269, pp. 513–519, 2018.

[11] S. Xie, R. Wickham, and L. D. Nghiem, 'Synergistic effect from anaerobic co-digestion of sewage sludge and organic wastes', *International Biodeterioration & Biodegradation*, vol. 116, pp. 191–197, 2017.

[12] Md. N. I. Siddique and Z. Ab. Wahid, 'Achievements and perspectives of anaerobic co-digestion: A review', *Journal of Cleaner Production*, vol. 194, pp. 359–371, Sep. 2018.

[13] T. Xie, S. Xie, M. Sivakumar, and L. D. Nghiem, 'Relationship between the synergistic/antagonistic effect of anaerobic co-digestion and organic loading', *International Biodeterioration & Biodegradation*, vol. 124, pp. 155–161, 2017.

[14] Y. Ren *et al.*, 'A comprehensive review on food waste anaerobic digestion: Research updates and tendencies', *Bioresource Technology*, vol. 247, pp. 1069–1076, Jan. 2018.

[15] V. Cabbai, M. Ballico, E. Aneggi, and D. Goi, 'BMP tests of source selected OFMSW to evaluate anaerobic digestion with sewage sludge', *Waste Management*, vol. 2013, pp. 1626–1632, 2013.

[16] K. Koch, M. Plabst, A. Schmidt, B. Helmreich, and J. E. Drewes, 'Co-digestion of food waste in a municipal wastewater treatment plant: Comparison of batch tests and full-scale experiences', *Waste Management*, vol. 47, pp. 28–33, 2016.

[17] M. Kim, M. M. I. Chowdhury, G. Nakhla, and M. Keleman, 'Synergism of co-digestion of food wastes with municipal wastewater treatment biosolids', *Waste Management*, vol. 61, pp. 473–483, Mar. 2017.

[18] C. Liu, H. Li, Y. Zhang, and C. Liu, 'Improve biogas production from low-organic-content sludge through high-solids anaerobic co-digestion with food waste', *Bioresource Technology*, vol. 219, pp. 252–260, 2016.

[19] C. Liu and H. Li, 'Resistance of high-solids anaerobic co-digestion of food waste and sewage sludge to sodium chloride', in *Treatment of Sewage sludge*, Beijing, China, 2018.
[20] H. Guven, M. E. Ersahin, R. K. Dereli, H. Ozgun, I. Isik, and I. Ozturk, 'Energy recovery potential of anaerobic digestion of excess sludge from high-rate activated sludge systems co-treating municipal wastewater and food waste', *Energy*, vol. 172, pp. 1027–1036, Apr. 2019.
[21] A. E. Maragkaki, I. Vasileiadis, M. Fountoulakis, A. Kyriakou, K. Lasaridi, and T. Manios, 'Improving biogas production from anaerobic co-digestion of sewage sludge with a thermal dried mixture of food waste, cheese whey and olive mill wastewater', *Waste Management*, vol. 71, pp. 644–651, Jan. 2018.
[22] N. Hamzawi, K. J. Kennedy, and D. D. McLean, 'Anaerobic digestion of co-mingled municipal solid waste and sewage sludge', *Water Science and Technology*, vol. 38, no. 2, pp. 127–132, Jan. 1998.
[23] P. Sosnowski, A. Wieczorek, and S. Ledakowicz, 'Anaerobic co-digestion of sewage sludge and organic fraction of municipal solid wastes', *Advances in Environmental Research*, vol. 7, no. 3, pp. 609–616, May 2003.
[24] V. Cabbai, N. De Bortoli, and D. Goi, 'Pilot plant experience on anaerobic codigestion of source selected OFMSW and sewage sludge', *Waste Management*, vol. 49, pp. 47–54, 2016.
[25] A. Mahdy, L. Mendez, M. Ballesteros, and C. González-Fernández, 'Algaculture integration in conventional wastewater treatment plants: Anaerobic digestion comparison of primary and secondary sludge with microalgae biomass', *Bioresource Technology*, vol. 184, pp. 236–244, May 2015.
[26] M. Wang, A. K. Sahu, B. Rusten, and C. Park, 'Anaerobic co-digestion of microalgae Chlorella sp. and waste activated sludge', *Bioresource Technology*, vol. 142, pp. 585–590, Aug. 2013.
[27] J. Lauwers, L. Appels, I. P. Thompson, J. Degrève, J. F. Van Impe, and R. Dewil, 'Mathematical modelling of anaerobic digestion of biomass and waste: Power and limitations', *Progress in Energy and Combustion Science*, vol. 39, no. 4, pp. 383–402, Aug. 2013.
[28] A. Donoso-Bravo, J. Mailier, C. Martin, J. Rodríguez, C. A. Aceves-Lara, and A. V. Wouwer, 'Model selection, identification and validation in anaerobic digestion: A review', *Water Research*, vol. 45, no. 17, pp. 5347–5364, Nov. 2011.
[29] K. Boe, D. J. Batstone, J.-P. Steyer, and I. Angelidaki, 'State indicators for monitoring the anaerobic digestion process', *Water Research*, vol. 44, no. 20, pp. 5973–5980, Dec. 2010.
[30] M. de Gracia, P. Grau, E. Huete, J. Gómez, J. L. García-Heras, and E. Ayesa, 'New generic mathematical model for WWTP sludge digesters operating under aerobic and anaerobic conditions: Model building and experimental verification', *Water Research*, vol. 43, no. 18, pp. 4626–4642, Oct. 2009.
[31] P. Grau, P. Vanrolleghem, and E. Ayesa, 'BSM2 Plant Wide Model construction and comparative analysis with other methodologies for integrated modeling', *Water Science and Technology*, vol. 58, no. 8, pp. 57–65, 2007.
[32] A. Donoso-Bravo, S. I. Pérez-Elvira, and F. Fdz-Polanco, 'Application of simplified models for anaerobic biodegradability tests. Evaluation of pre-treatment processes', *Chemical Engineering Journal*, vol. 160, no. 2, pp. 607–614, Jun. 2010.
[33] K. Koch and J. E. Drewes, 'Alternative approach to estimate the hydrolysis rate constant of particulate material from batch data', *Applied Energy*, vol. 120, pp. 11–15, May 2014.
[34] V. A. Vavilin, B. Fernandez, J. Palatsi, and X. Flotats, 'Hydrolysis kinetics in anaerobic degradation of particulate organic material: An overview', *Waste Management*, vol. 28, no. 6, pp. 939–951, Jan. 2008.
[35] S. Strömberg, M. Nistor, and J. Liu, 'Early prediction of Biochemical Methane Potential through statistical and kinetic modelling of initial gas production', *Bioresource Technology*, vol. 176, pp. 233–241, Jan. 2015.
[36] A. Mottet *et al.*, 'Estimating anaerobic biodegradability indicators for waste activated sludge', *Chemical Engineering Journal*, vol. 160, no. 2, pp. 488–496, Jun. 2010.

[37] C. Da Silva, S. Astals, M. Peces, J. L. Campos, and L. Guerrero, 'Biochemical methane potential (BMP) tests: Reducing test time by early parameter estimation', *Waste Management*, vol. 71, pp. 19–24, Jan. 2018.
[38] T. Hidaka, F. Wang, and J. Tsumori, 'Comparative evaluation of anaerobic digestion for sewage sludge and various organic wastes with simple modeling', *Waste Management*, vol. 43, pp. 144–151, Sep. 2015.
[39] G. Kiely, G. Tayfur, C. Dolan, and K. Tanji, 'Physical and mathematical modelling of anaerobic digestion of organic wastes', *Water Research*, vol. 31, no. 3, pp. 534–540, Mar. 1997.
[40] S. García-Gen, J. Rodríguez, and J. M. Lema, 'Control strategy for maximum anaerobic co-digestion performance', *Water Research*, vol. 80, pp. 209–216, Sep. 2015.
[41] D. J. Batstone *et al.*, *Anaerobic Digestion Model No.1 (ADM1) IWA Scientific and Technical Report No. 13*. London: IWA Publishing, 2002.
[42] C. Rosén and U. Jeppsson, 'Aspects on ADM1 implementation within the BSM2 framework'. 28-Nov-2006.
[43] A. M. Aboulfotoh, 'ADM1 simulation of the mesophilic anaerobic digestion of mixture of primary and secondary sludge treated by effective microorganisms', *International Journal of Engineering Research & Technology (IJERT)*, vol. 2, no. 10, Oct. 2013.
[44] S. Astals, M. Esteban-Gutiérrez, T. Fernandez-Arévalo, E. Aymerich, J. L. Garcìa-Heras, and J. Mata-Alvarez, 'Anaerobic digestion of seven different sewage sludges: A biodegradability and modelling study', *Water Research*, vol. 47, pp. 6033–6043, 2013.
[45] M. de Gracia, L. Sancho, J. L. Garcìa-Heras, P. Vanrolleghem, and E. Ayesa, 'Mass and charge conservation check in dynamic models: Application to the new ADM1 model', *Water Science and Technology*, vol. 53, no. 1, pp. 225–240, 2006.
[46] E. Huete, M. de Gracia, E. Ayesa, and J. L. Garcìa-Heras, 'ADM1-based methodology for the characterisation of the influent sludge in anaerobic reactors', *Water Science and Technology*, vol. 54, no. 4, pp. 157–166, 2006.
[47] R. Girault *et al.*, 'A waste characterisation procedure for ADM1 implementation based on degradation kinetics', *Water Research*, vol. 46, no. 13, pp. 4099–4110, Sep. 2012.
[48] D. Poggio, M. Walker, W. Nimmo, L. Ma, and M. Pourkashanian, 'Modelling the anaerobic digestion of solid organic waste – Substrate characterisation method for ADM1 using a combined biochemical and kinetic parameter estimation approach', *Waste Management*, vol. 53, pp. 40–54, Jul. 2016.
[49] T. S. O. Souza, A. Carvajal, A. Donoso-Bravo, M. Peña, and F. Fdz-Polanco, 'ADM1 calibration using BMP tests for modeling the effect of autohydrolysis pretreatment on the performance of continuous sludge digesters', *Water Research*, vol. 47, no. 9, pp. 3244–3254, Jun. 2013.
[50] V. Razaviarani and I. D. Buchanan, 'Calibration of the Anaerobic Digestion Model No. 1 (ADM1) for steady-state anaerobic co-digestion of municipal wastewater sludge with restaurant grease trap waste', *Chemical Engineering Journal*, vol. 266, pp. 91–99, Apr. 2015.
[51] S. Astals, D. J. Batstone, S. Tait, and P. D. Jensen, 'Development and validation of a rapid test for anaerobic inhibition and toxicity', *Water Research*, vol. 81, pp. 208–215, Sep. 2015.
[52] A. Hussain and S. K. Dubey, 'Specific methanogenic activity test for anaerobic degradation of influents', *Appl Water Sci*, vol. 7, no. 2, pp. 535–542, May 2017.
[53] H. Theil, *Economic Forecasts and Policy*, 2nd revised. Amsterdam: North Holland Publishing Co., 1961.

Appendix A

The main content of ADM1 is reported in this section [41]. All the biochemical rate coefficients and the kinetic rate equations for soluble and particulate components are shown in the Petersen matrix (Table A.2 and A.3).

The inhibition functions in the Petersen matrix are as follows:

$$I_{pH} = \begin{cases} exp\left(-3\left(\frac{pH - pH_{UL}}{pH_{UL} - pH_{LL}}\right)^2\right) \; if \; pH < pH_{UL} \\ 1 \; otherwise \end{cases}$$

$$I_{IN,lim} = \frac{1}{1 + {K_{S,IN}}/{S_{IN}}}$$

$$I_{h2} = \frac{1}{1 + {S_{h2}}/{K_I}}$$

$$I_{NH3,Xac} = \frac{1}{1 + {S_{nh3}}/{K_{I,nh3}}}$$

The differential-algebraic set of equations for the calculation of acid-base equilibrium is as follows:

Table A. 1 Acid-base equilibria algebraic equation set

Equation	**Unknow algebraic**
$\boldsymbol{S_{delta_{ions}} + S_{nh4_{ion}} + S_{h_{ion}} - S_{hco3_{ion}} - \frac{S_{ac_{ion}}}{64} - \frac{S_{pro_{ion}}}{112} - \frac{S_{bu_{ion}}}{160} - \frac{S_{va_{ion}}}{208} - S_{oh_{ion}} = 0}$	$S_{h_{ion}}$
$\boldsymbol{S_{oh_{ion}} - \frac{K_w}{S_{h_{ion}}} = 0}$	$S_{oh_{ion}}$
$\boldsymbol{S_{va_{ion}} - \frac{K_{a,va} S_{va}}{K_{a,va} + S_{h_{ion}}} = 0}$	$S_{va_{ion}}$
$\boldsymbol{S_{bu_{ion}} - \frac{K_{a,bu} S_{bu}}{K_{a,bu} + S_{h_{ion}}} = 0}$	$S_{bu_{ion}}$
$\boldsymbol{S_{pro_{ion}} - \frac{K_{a,pro} S_{pro}}{K_{a,pro} + S_{h_{ion}}} = 0}$	$S_{pro_{ion}}$
$\boldsymbol{S_{ac_{ion}} - \frac{K_{a,ac} S_{ac}}{K_{a,ac} + S_{h_{ion}}} = 0}$	$S_{ac_{ion}}$
$\boldsymbol{S_{hco3_{io3}} - \frac{K_{a,co2} S_{IC}}{K_{a,co2} + S_{h_{ion}}} = 0}$	$S_{hco3_{io3}}$

Equation	**Unknow algebraic**
$\boldsymbol{S_{nh4_{ion}} - \frac{S_{h_{ion}} S_{IN}}{K_{a,nh4} + S_{h_{ion}}} = 0}$	$S_{nh4_{ion}}$
$\boldsymbol{S_{IC} - S_{co2} - S_{hco3_{ion}} = 0}$	S_{co2}
$\boldsymbol{S_{IN} - S_{nh3} - S_{nh4_{ion}} = 0}$	S_{nh3}

In this study, the set of equation was slightly modified in the implementation in AQUASIM 2.0. The equilibrium of *S_hco3_ion* was re-written as a dynamic process for the variable *S_co2* (stoichiometric coefficient +1) and *S_IC* (-1) with kinetic rate as follows:

$$k_{AB_{co2}} * (S_{IC} * S_{h_{ion}} - (K_{a_{co2}} + S_{h_{ion}}) * S_{co2})$$

Therefore, *S_hco3_ion* was defined as the unknow algebraic in the balance of carbon ions.

In the original ADM1, dynamic gas transfer equations were suggested to be used to describe liquid-gas transfer. However, in the implementation in AQUASIM 2.0 the Henry's law was adopted as it could be defined in the diffusive link:

$$K_H \, p_{gas} - S_{liq} = 0$$

With S_{liq} was the liquid phase concentration of each component expresses in molar concentration (methane, carbon dioxide and hydrogen); p_{gas} was the gas phase partial pressure of each component (bar); and K_H is the Henry's law coefficient ($M \cdot bar^{-1}$). Despite that, AQUASIM 2.0 could simulate only systems in the liquid phase. Therefore, the partial pressure term in the Henry's law was substituted with the corresponding molar concentration in the gas phase. The partial pressure was calculated by means of the perfect gas equation consecutively:

$$p_{gas} = S_{gas} \cdot RT_{operation}$$

For methane and hydrogen, the formula was corrected by the stoichiometric COD coefficients (64 and 16 $kg_{COD}/kmol$, respectively). Furthermore, in AQUASIM 2.0 the exchange coefficient $k_L a$ was added in the definition of the diffusive link. As recommended in the report by the IWA Task Group, the same coefficient was used for all three gases because their diffusivities are similar.

$\nu_{i,j}$) and the kinetic rate equations (ρ_j) for soluble components (i = 1-12)

	Component →	*i*	1	2	3	4	5	6	7	8	9	10	11	12	Rate (ρ_j, kg COD.m^{-3}.d^{-1})
j	Process ↓		S_{su}	S_{aa}	S_{fa}	S_{va}	S_{bu}	S_{pro}	S_{ac}	S_{h2}	S_{ch4}	S_{ic}	S_{in}	S_{I}	
	Monosaccharides (kgCOD.m^{-3})														
	Amino acids (kgCOD.m^{-3})														
	Long chain fatty acids (kgCOD.m^{-3})														
	Total valerate (kgCOD.m^{-3})														
	Total butyrate (kgCOD.m^{-3})														
	Total propionate (kgCOD.m^{-3})														
	Total acetate (kgCOD.m^{-3})														
	Hydrogen gas (kgCOD.m^{-3})														
	Methane gas (kgCOD.m^{-3})														
	Inorganic carbon (kmoleC.m^{-3})														
	Inorganic nitrogen (kmoleN.m^{-3})														
	Soluble inerts (kgCOD.m^{-3})														
1	Disintegration													$f_{sI,xc}$	$k_{dis} X_c$
2	Hydrolysis carbohydrates		1												$k_{hyd,ch} X_{ch}$
3	Hydrolysis of proteins			1											$k_{hyd,pr} X_{pr}$
4	Hydrolysis of lipids		$1-f_{fa,li}$		$1-f_{fa,li}$										$k_{hyd,li} X_{li}$
5	Uptake of sugars		−1				$(1-Y_{su})f_{bu,su}$	$(1-Y_{su})f_{pro,su}$	$(1-Y_{su})f_{ac,su}$	$(1-Y_{su})f_{h2,su}$		$-\sum_{i=0,11-24} C_i v_{i,5}$	$-(Y_{su}) N_{bac}$		$k_{m,su} \frac{S_{su}}{K_S + S_{su}} X_{su} I_1$
6	Uptake of amino acids			−1		$(1-Y_{aa})f_{va,aa}$	$(1-Y_{aa})f_{bu,aa}$	$(1-Y_{aa})f_{pro,aa}$	$(1-Y_{aa})f_{ac,aa}$	$(1-Y_{aa})f_{h2,aa}$		$-\sum_{i=1-9,11-24} C_i v_{i,6}$	$N_{aa}-(Y_{aa}) N_{bac}$		$k_{m,aa} \frac{S_{aa}}{K_S + S_{aa}} X_{aa} I_1$
7	Uptake of LCFA				−1				$(1-Y_{fa})$ 0.7	$(1-Y_{fa})$ 0.3			$-(Y_{fa}) N_{bac}$		$k_{m,fa} \frac{S_{fa}}{K_S + S_{fa}} X_{fa} I_2$
8	Uptake of valerate					−1		$(1-Y_{c4})$ 0.54	$(1-Y_{c4})$ 0.31	$(1-Y_{c4})$ 0.15			$-(Y_{c4}) N_{bac}$		$k_{m,c4} \frac{S_{va}}{K_S + S_{va}} X_{c4} \frac{1}{1+S_{bu}/S_{bu}} \frac{1}{1+S_{pro}/S_{pro}} \frac{1}{1+S_{ac}/S_{ac}} I_2$
9	Uptake of butyrate						−1		$(1-Y_{c4})$ 0.8	$(1-Y_{c4})$ 0.2			$-(Y_{c4}) N_{bac}$		$k_{m,c4} \frac{S_{bu}}{K_S + S_{bu}} X_{c4} \frac{1}{1+S_{va}/S_{va}} \frac{1}{1+S_{pro}/S_{pro}} \frac{1}{1+S_{ac}/S_{ac}} I_2$
10	Uptake of propionate							−1	$(1-Y_{pro})$ 0.57	$(1-Y_{pro})$ 0.43		$-\sum_{i=1-9,11-24} C_i v_{i,10}$	$-(Y_{pro}) N_{bac}$		$k_{m,pro} \frac{S_{pro}}{K_S + S_{pro}} X_{pro} I_2$
11	Uptake of acetate								−1		$(1-Y_{ac})$	$-\sum_{i=1-9,11-24} C_i v_{i,11}$	$-(Y_{ac}) N_{bac}$		$k_{m,ac} \frac{S_{ac}}{K_S + S_{ac}} X_{ac} I_3$
12	Uptake of hydrogen									−1	$(1-Y_{h2})$	$-\sum_{i=1-9,11-24} C_i v_{i,12}$	$-(Y_{h2}) N_{bac}$		$k_{m,h2} \frac{S_{h2}}{K_S + S_{h2}} X_{h2} I_1$
13	Decay of X_{su}														$k_{dec,Xsu} X_{su}$
14	Decay of X_{aa}														$k_{dec,Xaa} X_{aa}$
15	Decay of X_{fa}														$k_{dec,Xfa} X_{fa}$
16	Decay of X_{c4}														$k_{dec,Xc4} X_{c4}$
17	Decay of X_{pro}														$k_{dec,Xpro} X_{pro}$
18	Decay of X_{ac}														$k_{dec,Xac} X_{ac}$
19	Decay of X_{h2}														$k_{dec,Xh2} X_{h2}$
	Inhibition factors:														$I_1 = I_{pH,UL,lim} \cdot I_{IN,lim}$ $I_2 = I_{pH,UL,lim} \cdot I_{h2}$ $I_3 = I_{pH,UL,lim} \cdot I_{NH3,Xac}$

ents ($v_{i,j}$) and the kinetic rate equations (ρ_j) for particulate components (i = 13-24)

	Component →	*i*	13	14	15	16	17	18	19	20	21	22	23	24	Rate (ρ_j, kg COD.m^{-3}.d^{-1})
j	Process ↓		X_c	X_{ch}	X_{pr}	X_{li}	X_{su}	X_{aa}	X_{fa}	X_{c4}	X_{pro}	X_{ac}	X_{h2}	X_I	
			Composites (kgCOD·m^{-3})	Carbohydrates (kgCOD·m^{-3})	Proteins (kgCOD·m^{-3})	Lipids (kgCOD·m^{-3})	Sugar degraders (kgCOD·m^{-3})	Amino acid degraders (kgCOD·m^{-3})	LCFA degraders (kgCOD·m^{-3})	Valerate and butyrate degraders (kgCOD·m^{-3})	Propionate degraders (kgCOD·m^{-3})	Acetate degraders (kgCOD·m^{-3})	Hydrogen degraders (kgCOD·m^{-3})	Particulate inerts (kgCOD·m^{-3})	Inhibition factors: $I_1 = I_{pH7IN,lim}$ $I_2 = I_{pH7IN,lim}.I_{h2}$ $I_3 = I_{pH7IN,lim}.I_{NH3,xac}$
1	Disintegration		-1	$f_{ch,xc}$	$f_{pr,xc}$	$f_{li,xc}$								$f_{xI,xc}$	$k_{dis}X_c$
2	Hydrolysis carbohydrates			-1											$k_{hyd,ch}X_{ch}$
3	Hydrolysis of proteins				-1										$k_{hyd,pr}X_{pr}$
4	Hydrolysis of lipids					-1									$k_{hyd,li}X_{li}$
5	Uptake of sugars						Y_{su}								$k_{m,su}\frac{S_{su}}{K_S+S_{su}}X_{su}I_1$
6	Uptake of amino acids							Y_{aa}							$k_{m,aa}\frac{S_{aa}}{K_S+S_{aa}}X_{aa}I_1$
7	Uptake of LCFA								Y_{fa}						$k_{m,fa}\frac{S_{fa}}{K_S+S_{fa}}X_{fa}I_2$
8	Uptake of valerate									Y_{c4}					$k_{m,c4}\frac{S_{va}}{K_S+S_{va}}X_{c4}\frac{1}{1+S_{va}/S_{ac}}I_1$
9	Uptake of butyrate									Y_{c4}					$k_{m,c4}\frac{S_{bu}}{K_S+S_{bu}}X_{c4}\frac{1}{1+S_{bu}/S_{ac}}I_1$
10	Uptake of propionate										Y_{pro}				$k_{m,pr}\frac{S_{pro}}{K_S+S_{pro}}X_{pro}I_2$
11	Uptake of acetate											Y_{ac}			$k_{m,ac}\frac{S_{ac}}{K_S+S_{ac}}X_{ac}I_3$
12	Uptake of hydrogen												Y_{h2}		$k_{m,h2}\frac{S_{h2}}{K_S+S_{h2}}X_{h2}I_1$
13	Decay of X_{su}		1												$k_{dec,Xsu}X_{su}$
14	Decay of X_{aa}		1					-1							$k_{dec,Xaa}X_{aa}$
15	Decay of X_{fa}		1						-1						$k_{dec,Xfa}X_{fa}$
16	Decay of X_{c4}		1							-1					$k_{dec,Xc4}X_{c4}$
17	Decay of X_{pro}		1								-1				$k_{dec,Xpro}X_{pro}$
18	Decay of X_{ac}		1									-1			$k_{dec,Xac}X_{ac}$
19	Decay of X_{h2}		1										-1		$k_{dec,Xh2}X_{h2}$

Appendix B

The mixtures of nutrients that can be added to the test bottles in the anaerobic biodegradability test were prepared as follow.

Table B. 1 Ingredients of mother solution A

Substance	*Reagentary code*	*Mass (g)*	*Package number*
KH_2PO_4	AR35	2,7	AR35
$Na_2HPO_4*12H_2O$	AR40	11,2	AR40
NH_4Cl	AR23	5,3	AR23

Table B. 2 Ingredients of mother solution B

Substance	*Reagentary code*	*Mass (g)*	*Package number*
$CaCl_2*2H_2O$	AR24	0,75	AR24
$MgCl_2*6H_2O$	AR28	1,0	AR28
$FeCl_2*4H_2O$	AR26	0,2	AR26

Table B. 3 Ingredients of mother solution C

Substance	*Mass (g)*
$MnCl_2*4H_2O$	0,05
H_3BO_3	0,005
$ZnCl_2$	0,005
$CuCl_2$	0,003
$Na_2MoO_4*2H_2O$	0,001
$CoCl_2*6H_2O$	0,1
$NiCl_2*6H_2O$	0,01
Na_2SeO_3	0,005

In a flask for each mixture, add distilled water to the mother solution A, B and C in order to obtain final volume of 0.5 L, 0.5 L and 1 L, respectively.
In the bottles with the samples for the test, solution A and B must be added due to 5% of the final test volume; solution C must be added due to 1% of the final test volume.

Appendix C

List of all the parameters that have been assumed as default from the report of Rosén and Jeppsson [42].

Table C. 1 ADM1 benchmark model, stoichiometric parameter values (on the left of the table) and biochemical parameter values (on the right)

Parameter	Value	Unit	Parameter	Value	Unit
N_Xc	0,02	$kmol_N/kg_{COD}$	**kdec_h2**	0,02	d^{-1}
C_aa	0,03	$kmol_C/kg_{COD}$	**kdec_Xaa**	0,02	d^{-1}
C_ac	0,0313	$kmol_C/kg_{COD}$	**kdec_Xac**	0,02	d^{-1}
C_biom	0,0313	$kmol_C/kg_{COD}$	**kdec_Xc4**	0,02	d^{-1}
C_bu	0,025	$kmol_C/kg_{COD}$	**kdec_Xfa**	0,02	d^{-1}
C_ch	0,0313	$kmol_C/kg_{COD}$	**kdec_Xpro**	0,02	d^{-1}
C_ch4	1/64	$kmol_C/kg_{COD}$	**kdec_Xsu**	0,02	d^{-1}
C_fa	0,0217	$kmol_C/kg_{COD}$	**kdis**	0,5	d^{-1}
C_li	0,022	$kmol_C/kg_{COD}$	**khyd_ch**	10	d^{-1}
C_pr	0,03	$kmol_C/kg_{COD}$	**khyd_li**	10	d^{-1}
C_pro	0,0268	$kmol_C/kg_{COD}$	**khyd_pr**	10	d^{-1}
C_SI	0,03	$kmol_C/kg_{COD}$	**KI_h2_c4**	1E-05	d^{-1}
C_su	0,0313	$kmol_C/kg_{COD}$	**KI_h2_fa**	5E-06	$kgCOD/m^3$
C_va	0,024	$kmol_C/kg_{COD}$	**KI_h2_pro**	3,5E-06	$kgCOD/m^3$
C_Xc	0,0279	$kmol_C/kg_{COD}$	**KI_nh3**	0,0018	M
C_XI	0,03	$kmol_C/kg_{COD}$	**km_aa**	50	d^{-1}
f_ac_aa	0,4	-	**km_ac**	8	d^{-1}
f_ac_su	0,41	-	**km_c4**	20	d^{-1}
f_bu_aa	0,26	-	**km_fa**	6	d^{-1}
f_bu_su	0,13	-	**km_h2**	35	d^{-1}
f_fa_li	0,95	-	**km_pro**	13	d^{-1}

Parameter	Value	Unit	Parameter	Value	Unit
f_h2_aa	0,06	-	**km_su**	30	d^{-1}
f_h2_su	0,19	-	**Ks_aa**	0,3	$kgCOD/m^3$
f_pro_aa	0,05	-	**Ks_ac**	0,15	$kgCOD/m^3$
f_pro_su	0,27	-	**Ks_c4**	0,2	M
f_va_aa	0,23	-	**Ks_fa**	0,4	$kgCOD/m^3$
N_aa	0,007	$kmol_N/kg_{COD}$	**Ks_h2**	7E-06	$kgCOD/m^3$
N_biom	0,08/14	$kmol_N/kg_{COD}$	**Ks_IN**	1E-04	M
N_I	0,06/14	$kmol_N/kg_{COD}$	**Ks_pro**	0,1	$kgCOD/m^3$
Y_aa	0,08	-	**Ks_su**	0,5	$kgCOD/m^3$
Y_ac	0,05	-	**pH_LL_aa**	4	-
Y_c4	0,06	-	**pH_LL_ac**	6	-
Y_fa	0,06	-	**pH_LL_h2**	5	-
Y_h2	0,06	-	**pH_UL_aa**	5,5	-
Y_pro	0,04	-	**pH_UL_ac**	7	-
Y_su	0,1	-	**pH_UL_h2**	6	-

Table C. 2 ADM1 benchmark model, physiochemical parameter values; Van't Hoff temperature correction has been applied if required

Parameter	Value	Unit
R	0,08314	bar M^{-1} K^{-1}
T	308	K
Ka_ac	10^ (-4,76)	M
Ka_bu	10^ (-4,82)	M
Ka_co2	$10^{6,35}\exp\left(\frac{7646}{R*100}\left(\frac{1}{298}-\frac{1}{T}\right)\right)$	M
Ka_IN	$10^{9,25}\exp\left(\frac{51965}{R*100}\left(\frac{1}{298}-\frac{1}{T}\right)\right)$	M
Ka_pro	10^ (-4,88)	M
Ka_va	10^ (-4,86)	M

Parameter	Value	Unit
kAB_co2	1E-14	$M^{-1}\ d^{-1}$
KH_ch4	$0{,}0014 \cdot \exp\left(\frac{-14240}{R*100}\left(\frac{1}{298}-\frac{1}{T}\right)\right)$	$M_{liq}\ bar^{-1}$
KH_co2	$0{,}035 \cdot \exp\left(\frac{-19410}{R*100}\left(\frac{1}{298}-\frac{1}{T}\right)\right)$	$M_{liq}\ bar^{-1}$
KH_h2	$7{,}8e-4 \cdot \exp\left(\frac{-4180}{R*100}\left(\frac{1}{298}-\frac{1}{T}\right)\right)$	$M_{liq}\ bar^{-1}$
kLa	200	d^{-1}
Kw	$\exp\left(\frac{55900}{R*100}\left(\frac{1}{298}-\frac{1}{T}\right)\right)$	M
P_atm	1,0313	bar
p_h2o	$0{,}0313 \cdot \exp\left(5290\left(\frac{1}{298}-\frac{1}{T}\right)\right)$	bar

Appendix D

As reported in ADM1, the gas flow exiting the headspace of the anaerobic reactor can be calculated by a control loop in pressure. The gas phase pressure must be calculated from partial pressures, and the flow calculated for restricted flow through an orifice. It is assumed an overpressure in the headspace.

$$P_{gas} = p_{gas_{h2}} + p_{gas_{ch4}} + p_{gas_{co2}} + p_{gas_{h2o}}$$

$$q_{gas} = k_p(P_{gas} - P_{atm})$$

With k_p equal to the pipe resistance coefficient ($m^3\ d^{-1}\ bar^{-1}$).

In the AQUASIM 2.0 system, the equation was corrected to obtain the gas flow rate at atmospheric pressure (like as in the AMPTS II system).

$$q_{gas} = \frac{P_{gas} - P_{atm}}{P_{atm}} \cdot k_p$$

The k_p value reported by Rosén and Jeppsson is equal to 50000 $m^3\ d^{-1}\ bar^{-1}$, but in the simulation of both the full-scale digester and the bench-scale tests the coefficient was set to 10000 $m^3\ d^{-1}\ bar^{-1}$, as found in literature.